Application of the assessment of right ventricular function by echocardiography in dogs with heart disease

(犬心疾患への心エコー図法を用いた右心室機能評価の応用)

Tomoya Morita

Laboratory of Veterinary Internal Medicine

Department of Veterinary Clinical Sciences

Graduate School of Veterinary Medicine

Hokkaido University

March 2018

Application of the assessment of right ventricular function by echocardiography in dogs with heart disease

(犬心疾患への心エコー図法を用いた右心室機能評価の応用)

Tomoya Morita

GENERAL ABBREVIATIONS

A wave	Transtricuspid valve late diastolic flow wave
A'_{TV}	Peak late diastolic tricuspid annular velocity
BP	Arterial blood pressure
CI	Cardiac index
CO	Cardiac output
CRI	Constant rate infusion
CV	Coefficient of variation
CVP	Central venous pressure
DPD	Dual pulsed-wave Doppler
ECG	Electrocardiography
E wave	Transtricuspid valve early diastolic flow wave
E'_{TV}	Peak early diastolic tricuspid annular velocity
FAC	Fractional area change
ICC	Intraclass correlation coefficient

LV	Left ventricle
Max dP/dt	The first derivatives of the maximum right ventricular pressure change
PAP	Pulmonary arterial pressure
PAWP	Pulmonary arterial wedge pressure
PH	Pulmonary hypertension
PVR	Pulmonary vascular resistance
RHC	Right heart catheterization
Rp/Rs	Pulmonary vascular resistance to systemic vascular resistance ratio
RTX	Right ventricular Tei index
RTX_{DPD}	Right ventricular Tei index derived from dual pulsed-wave Doppler
RTX_{PD}	Right ventricular Tei index derived from pulsed-wave Doppler
RTX_{TD}	Right ventricular Tei index derived from tissue Doppler

RV	Right ventricle
RVEDA	Right ventricular end-diastolic area
RVESA	Right ventricular end-systolic area
RVLS	Right ventricular longitudinal strain
RVP	Right ventricular pressure
RV-SD6	Standard deviation of the systolic shortening time of RV 6segments
SD	Standard deviation
SST	Systolic shortening time
STE	Speckle tracking echocardiography
S'_{TV}	Peak systolic tricuspid annular velocity
SVR	Systemic vascular resistance
TAPSE	Tricuspid annulus plane systolic excursion
Tau	Time constant of right ventricular relaxation
TD	Tissue Doppler

TABLE OF CONTENTS

CHAPTER 2

THE REPEATABILITY AND CHARACTERISTICS OF RIGHT VENTRICULAR LONGITUDINAL STRAIN IMAGING BY SPECKLE TRACKING ECHOCARDIOGRAPHY IN HEALTHY DOGS.....25

CHAPTER 3

CHANGES IN RIGHT VENTRICULAR FUNCTION ASSESSED BY ECHOCARDIOGRAPHY IN DOG MODELS OF RV PRESSURE-OVERLOAD 52

GENERAL INTRODUCTION

Heart failure is one of the most common clinical syndrome, and the most important cause of death in both humans and dogs. Echocardiography is a mainstay to assess the motion and structure of the heart in humans and dogs with heart disease, and has been used in diagnosis of heart failure, evaluation of the disease severity, and risk stratification. The main target of echocardiographic assessment in both humans and dogs has been left ventricle (LV) because LV is considered as a physiological important chamber.

On the other hand, the physiological importance of right ventricle (RV) has long been underestimated. Recently, it has been shown that the RV function assessed by magnetic resonance imaging and cardiac catheterization is closely associated with the hemodynamic deterioration and clinical outcome in human patients with not only right heart disease, such as pulmonary hypertension (PH)[1,2], but also left heart disease, such as mitral valvular disease[3], and dilated cardiomyopathy[4]. Furthermore, RV intraventricular dyssynchrony, abnormality of timing of RV contraction between free wall and septum, has been described in human patients with PH, and has been associated with more pronounced RV dysfunction and clinical worsening.[5,6] Therefore, the assessment of RV

function has recently garnered increasing interest in human medicine.

Magnetic resonance imaging and cardiac catheterization are invasive, expensive, and time consuming for serial assessment of RV function. In addition, anesthesia is necessary during these procedures in dogs. On the other hand, echocardiography is noninvasive, inexpensive, and does not require anesthesia. Thus, the assessment of RV function by echocardiography gain more interest in humans and veterinary medicine. However, accurate assessment of RV function by echocardiography is challenging because of its complex geometry and contractile properties. In current guidelines for the echocardiographic assessment of RV size and function, it is recommended to assess RV function by using multiple echocardiographic indices of RV function including the peak systolic tricuspid annulus velocity by tissue Doppler (S'_{TV}), tricuspid annulus plane systolic excursion by the M-mode (TAPSE), fractional area change (FAC), RV Tei index (RTX), and RV longitudinal strain (RVLS) derived from speckle tracking echocardiography (STE).[7,8] These echocardiographic indices have been examined in healthy dogs as well as clinical setting, and some of these indices have been shown to be impaired in dogs with PH compared with healthy dogs.[9–14] However, these parameters have some limitations; S'_{TV} and TAPSE can only assess regional tricuspid annulus and are angle-dependence, while FAC is experience-dependence and often shows poor

reproducibility.[7,8] Looking at these points, we focused on 2 echocardiographic indices of RV function which are angle-independent and unaffected by complex geometry; RTX and RVLS derived from STE.

RTX is an index of overall myocardial function, including systolic and diastolic performance.[15] An important limitation of the RTX obtained by conventional methods is it cannot be calculated in a single cardiac cycle that makes it being influenced by heart rate fluctuations (i.e., respiratory sinus arrhythmia). To overcome this limitation, we apply the dual pulsed-wave Doppler (DPD), which can simultaneously record Doppler signals at two different points simultaneously in one image.

STE is a novel quantitative method for assessment of the regional and global myocardial deformation in greyscale B-mode images. In humans, RVLS derived from STE, which is an index for assessing the RV systolic function, and the standard deviation of the systolic shortening time (SST) of RV 6segments (RV-SD6), which is an index for RV intraventricular dyssynchrony, has been applied for evaluating RV function and dyssynchrony.

However, there are a few studies on these echocardiographic indices of RV function in dogs. To our best knowledge, no reports on RTX derived from DPD (RTX_{DPD}) and only 2 reports on RVLS derived from STE exist to date.[16,17] These 2 reports on RVLS

indicated a high repeatability, provided a reference value of RVLS, and suggested the correlation between RVLS values and characteristics in healthy dogs.[16,17] In contrast, no report is available on RV-SD6 in dogs. Additionally, changes in these echocardiographic indices of RV function under an RV pressure-overload condition in dogs is unknown.

Considering the above background, this study was performed in 3 stages to establish the clinical utility of the echocardiographic indices of RV function in dogs with heart disease. In the first stage, the repeatability and reference value of RTX_{DPD} have established. In the second stage, the repeatability and reference value of RVLS and RV-SD6 by STE have established. In the third stage, the effect of RV pressure-overload on echocardiographic indices of RV function have determined.

CHAPTER 1

REPEATABILITY AND REPRODUCIBILITY OF RIGHT VENTRICULAR TEI INDEX VALUES DERIVED FROM THREE ECHOCARDIOGRAPHIC METHODS FOR EVALUATION OF CARDIAC FUNCTION IN DOGS

1. INTRODUCTION

RTX is an index of overall myocardial function, including systolic and diastolic performance.[15] This measurement involves a simple technique without geometric assumptions, and it correlates well with both the invasive systolic and diastolic function variables of RV in healthy dogs.[13] In addition, it has been shown that RTX is useful for predicting hemodynamic variables and monitoring disease severity in human patients with PH[18,19], and providing information on the severity and prognosis of dogs with cardiac disease.[13,14] To date, the RTX has been derived from pulsed-wave Doppler[15] and tissue Doppler echocardiography[20]. However, there is an important limitation in that the RTX derived from conventional pulsed-wave Doppler (RTX_{PD}) cannot be calculated in a single cardiac cycle; therefore, it is influenced by heart rate fluctuations (i.e., respiratory sinus arrhythmia). On the other hand, tissue Doppler can simultaneously record systolic and diastolic phases, but it was reported that RTX derived from tissue Doppler (RTX_{TD}) values were different from RTX_{PD} values in dogs.[21]

Dual pulsed-wave Doppler (DPD) can simultaneously record Doppler signals at two different points, setting two separate sample volumes in one image. Therefore, measurement of the RTX during the same cardiac cycle is possible, which may overcome

the limitation of measurement by pulsed-wave Doppler. In human medicine, it was demonstrated that the intra- and interobserver repeatability of RTX derived from DPD (RTX_{DPD}) were high.[22] In addition, RTX_{TD} values are higher than RTX_{PD} and RTX_{DPD} values.[22]

So far, in dogs, RTX measurement derived from DPD has not been applied to the evaluation of RV function, and therefore its repeatability remains unknown. In addition, degrees of agreement among RTX values derived from the 3 echocardiographic methods have not reported in dogs. In order to determine whether differences in data reflect clinically important changes resulting from disease progression in an individual patient, it is necessary to evaluate the repeatability of RTX measurement, and to validate statistical relationship among RTX derived from 3 different echocardiographic methods.

Thus, the goal of chapter 1 was to assess the repeatability of the RTX measurement derived from 3 different echocardiographic methods in healthy dogs, and to validate the relationship among RTX values derived from 3 different echocardiographic methods.

2. MATERIALS AND METHODS

2.1 Dogs

Six laboratory Beagles (two females, four males; 1-3 years; 9.5-13.0 kg) were used in this study. All dogs were determined to be healthy and have a normal heart anatomy and myocardial function, as determined on the basis of normal findings on complete physical examination, electrocardiography, and standard echocardiographic examinations (including M-mode, pulsed-wave Doppler, and color flow Doppler imaging). All procedures were approved by the Laboratory Animal Experimentation Committee, Graduate School of Veterinary Medicine, Hokkaido University (Approval No. 15-0087).

2.2 Echocardiographic measurements

Echocardiographic measurements were performed using an ultrasound machine (HI VISION Preirus; Hitachi Medical Corporation, Chiba, Japan) equipped with a 3 to 7 MHz sector probe (EUP-S52; Hitachi Medical Corporation, Chiba, Japan). All dogs were examined while manually restrained in left lateral recumbent positions without sedation. An ECG trace (lead II) was recorded simultaneously with echocardiographic imaging and automatically measured heart rate. RTX was calculated using DPD, pulsed-wave Doppler,

and tissue Doppler by two echocardiogarphers. RTX was defined as the sum of the isovolumic contraction time (ICT) and isovolumic relaxation time (IRT) divided by ejection time (ET) (Figure 1). For each RTX, the mean values of three different cardiac cycles were used to assess the repeatability. Each RTX was calculated after image acquisition.

To calculate RTX_{DPD}, tricuspid inflow and pulmonary artery (PA) flow were measured simultaneously using DPD with a left parasternal short-axis view, and ICT + IRT was derived by subtracting ET from the time of the cessation of the tricuspid valve A wave to the onset of the tricuspid valve E wave in one image (Figure 1 A).[22] ET was measured from the beginning of one to the beginning the next PA spectrum.

To calculate RTX_{PD}, firstly, tricuspid inflow was measured with a left parasternal short-axis view. Next, PA flow was measured with a left parasternal short-axis view. Finally, ICT + IRT was derived by subtracting ET from the time of the cessation of the tricuspid valve A wave to the onset of the tricuspid valve E wave using two different images (Figure 1 B, C).[23] No attempt was made to match R-R intervals for the in- and outflow signals because it is difficult to match RR intervals in clinical settings.

To calculate RTX_{TD}, the $S`_{TV}$, peak early diastolic tricuspid annular velocity ($E`_{TV}$), and peak late diastolic tricuspid annular velocity ($A`_{TV}$) were determined by tissue

Doppler with an apical 4-chamber view. Then, ICT + IRT was derived by subtracting the S`$_{TV}$ duration from the time from the end of A`$_{TV}$ to the onset of E`$_{TV}$ on the basis of tissue Doppler recordings (Figure 1 D).[7]

2.3 Statistical analysis

Power calculations for sample size determination were made on the basis of data from previous study.[24] Presuming a similar intraobserver within-day, intraobserver between-day, and interobserver intraclass correlation coefficient (ICC), it was estimated that a sample size of 6 dogs would be required in this study to provide a power of 90% to demonstrate ICC = 0.75[24], a null hypothesis of ICC = 0, with $\alpha = 0.05$, and the numbers of measurement is 3 times.[25] Statistical analyses were performed using computer software (JMP, version 8.0, SAS Institute Inc., Cary, NC, USA). Results are summarized as least square means (95% confidence intervals).

Statistical analyses programs were used to develop a linear mixed model, with measurement time (1 to 9 times), method (DPD, tissue Doppler, and pulsed-wave Doppler), and their interaction as categorical fixed effects, and dog identity as a random effect. The *F* test was performed to assess the effect of measurement time and method on RTX values. Multiple comparisons were made by obtaining the least square means by one observer's (KN) measurement and applying Tukey honest significant difference

(HSD) test to assess differences among methods. The all-pairs, Tukey HSD test allows significance tests of all combinations of pairs, and the resulting HSD intervals are greater than those provided with the Student pairwise *t* for least significant differences.

The following linear model was used for the variables in within- and between-day and interobserver variability analysis[26]:

$$Y_{ijkl} = \mu + Observer_i + Day_j + Dog_k + (Observer \times Dog)_{ik} + (Day \times Dog)_{jk} + \varepsilon_{ijkl}$$

where Y_{ijkl} was the first value measured for dog k on day j by observer i, μ was the general mean, $Observer_i$ was the differential effect (considered as fixed) of observer i, Dog_k was the differential effect of dog k, $(Observer \times Dog)_{ik}$ is the interaction term between the observer and dog, (Day × Dog) is the interaction term between day and dog, and ε_{ijkl} is the model error. The SD of within-day variability was estimated as the residual SD of the model, SD of between-day variability as the SD of the differential effect of day, and SD of interobserver variability as the SD of the differential effect of observer. The corresponding coefficients of variations (CV) were determined by dividing each SD by the mean.

The intraobserver within-day ICC was determined from data generated by the

same observer (KN); this echocardiographer evaluated 6 dogs 3 times repeatedly during the same day. The intraobserver between-day ICC was determined from data generated by 1 blinded observer (KN); on 3 different days, this echocardiographer made 3 evaluations of the 6 dogs. The interobserver ICC was determined from data generated by 2 blinded observers (KN, TM) on the same day; these echocardiographers evaluated 6 dogs 3 times repeatedly during the same day. Agreement was considered marked when CV < 20%[26,27] and ICC > 0.75[24].

Differences among measurements derived from the 3 methods were evaluated by use of Bland-Altman analysis, with modification for repeated measures as described elsewhere.[28] Mean difference (bias) and 95% limits of agreement were calculated. Differences among methods were considered significant when the 95% limits of agreement did not contain 0. Values of $P < 0.05$ were considered significant.

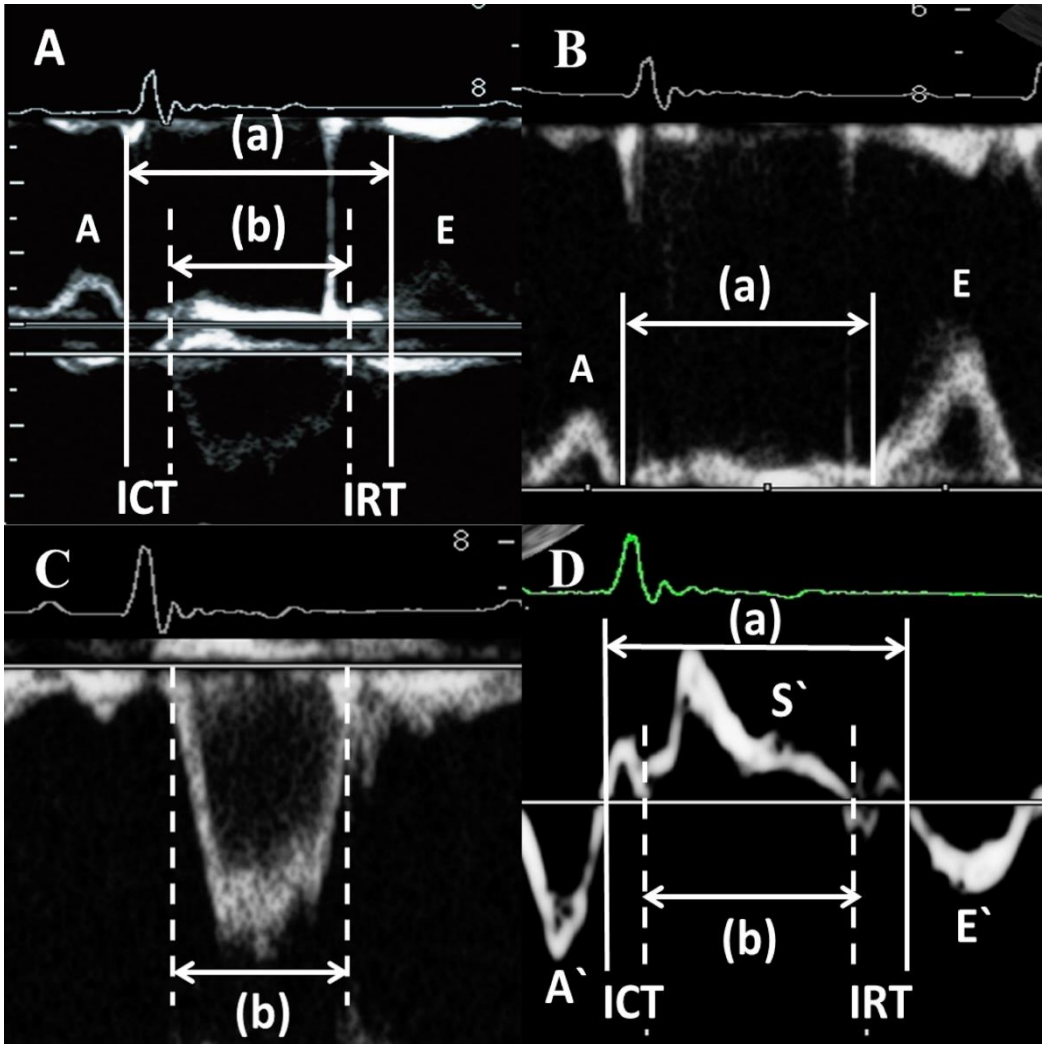

Figure 1. Echocardiographic images illustrating a technique used to measure RTX in dogs by means of DPD (A), pulsed-wave Doppler (B and C), and tissue Doppler (C) techniques. A－The upper waveform is tricuspid inflow, and lower waveform is pulmonary artery flow. B－Tricuspid inflow is shown. C－Pulmonary artery flow is shown. D－Tricuspid annular velocity is shown. The simultaneously recorded ECG appears at the top. For all calculations, RTX = (a – b)/b. a = interval from tricuspid valve closure to opening (pulsed-wave Doppler recordings) or the end of the A'_{TV} wave to the beginning of the E'_{TV} wave

(tissue Doppler recordings). A = transtricuspid valve late diastolic flow. A` = peak late diastolic tricuspid annular velocity. b = Ejection time or $S`_{TV}$ duration. E = transtricuspid valve early diastolic flow. E` = peak early diastolic tricuspid annular velocity. ICT = isovolumic contraction time. IRT = isovolumic relaxation time. S` = peak systolic tricuspid annular velocity.

3. RESULTS

Least square means obtained from linear mixed model for RTX and its components obtained using the 3 different methods by one observer are summarized in Table 1. The values of RTX_{TD} were higher than those of RTX_{DPD} and RTX_{PD}. In contrast, the values of RTX_{DPD} was not significantly different from those of RTX_{PD}. The tricuspid closure to opening time (TCO) and isovolumic time (the sum of ICT and IRT) derived from tissue Doppler were longer than respective values derived from the DPD and pulsed-wave Doppler methods. No difference in heart rate was identified among the 3 methods.

Bland-Altman analysis revealed that RTX_{TD} values were significantly higher than RTX_{DPD} and RTX_{PD} values (Figure 2). However, agreement was good between RTX_{DPD} and RTX_{PD} (Figure 2).

Intraobserver within- and between-day and interobserver CVs and ICCs of RTX derived from the 3 different methods are summarized in Table 2. The RTX_{DPD} had high (low CV and high ICC) within-day and interobserver but between-day repeatability was not high. The RTX_{TD} had high within-day repeatability, but between-day and interobserver repeatability were not high. The RTX_{PD} lacked high within- and between-

day repeatability and interobserver repeatability.

Table 1. Least square means (95% confidence intervals) RTX values as assigned to healthy adult Beagles (n = 6) by 1 observer using 3 echocardiographic methods and variables identified through mixed linear modeling as associated with those values.

	Dual pulsed-wave Doppler	Tissue Doppler	Pulsed-wave Doppler
RTX	0.27 (0.23-0.31)[a]	0.50 (0.46-0.54)[b]	0.25 (0.21-0.29)[a]
TCO (ms)	252 (236-268)[a]	286 (270-292)[b]	245 (229-261)[a]
Ejection time (ms)	199 (189-209)[a]	191 (181-201)[a]	196 (186-206)[a]
ICT + IRT (ms)	53 (43-63)[a]	95 (85-105)[b]	49 (39-59)[a]
HR (beats/min)	93 (77-109)[a]	91 (75-107)[a]	94 (78-110)[a]

ICT = isovolumic contraction time. IRT = isovolumic relaxation time. RTX = right ventricular Tei index. TCO = interval between tricuspid valve closure and opening.

[a, b]Values in the same row with different superscript letters are significantly ($P < 0.05$; Tukey`s HSD) different.

Table 2. Within- and between-day (1 observer) and interobserver (2 observers) CVs and ICCs for 3 echocardiographic methods of RTX measurement in healthy adult Beagles (n = 6) performed 3 times/d for 3 days.

Variable	**Within-day**		**Between-day**		**Interobserver**	
	CV (%)	**ICC**	**CV (%)**	**ICC**	**CV (%)**	**ICC**
DPD	6.1	0.77	8.4	0.73	3.5	0.83
Tissue Doppler	6.0	0.80	7.7	0.63	24.6	0.62
Pulsed-wave Doppler	20.7	0.62	20.7	0.35	19.1	0.65

Agreement was considered high when the CV was < 20% and the ICC was > 0.75.

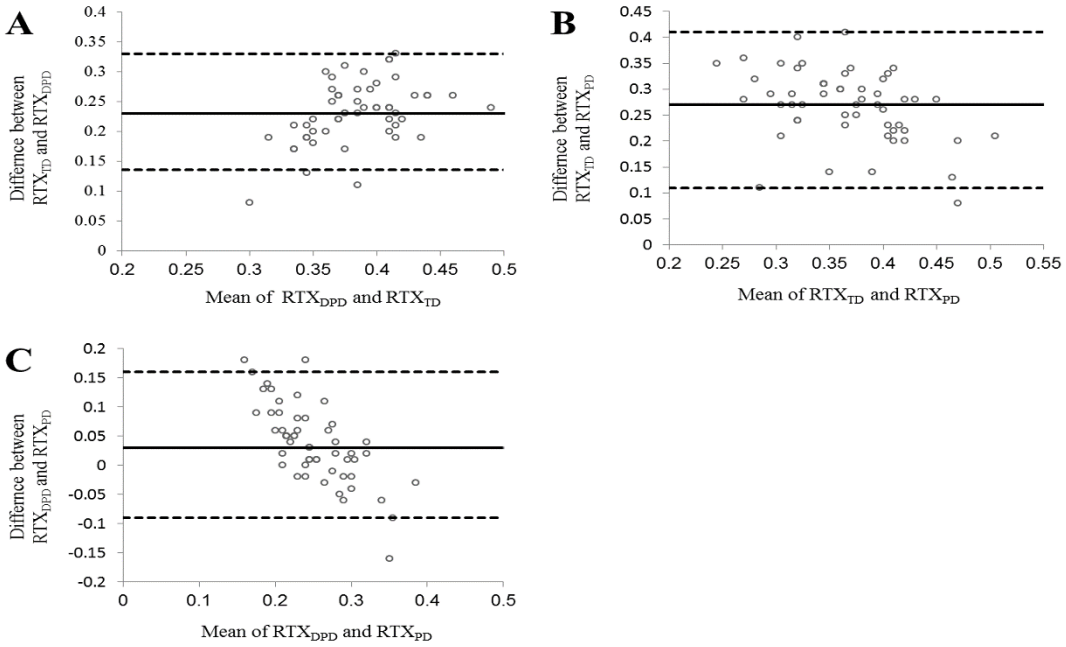

Figure 2. Bland-Altman plot of difference among 3 echocardiographic methods for RTX measurement in healthy adult Beagles (n = 6) by 1 observer. A－Bias (95% CI) between RTX_{TD} and RTX_{DPD} was 0.23 (0.18 to 0.28), B－Bias between RTX_{TD} and RTX_{PD} was 0.27 (0.19 to 0.35), C－Bias between RTX_{DPD} and RTX_{PD} was 0.04 (-0.03 to 0.10). Solid horizontal line represents the bias (mean difference), and the dashed lines above and below the solid line represent the 95% limits of agreement.

4. DISCUSSION

In the present study, the within-day and interobserver repeatability for RTX_{DPD} were high in a small number of healthy Beagles. To our knowledge, this study provides the first description of the repeatability of RTX_{DPD}, RTX_{PD}, and RTX_{TD}. Our results agree with previous reports in humans.[22] The DPD method allows simultaneous recording of Doppler signals at 2 points during the same cardiac cycle; therefore, RTX_{DPD} measurement is not influenced by heart rate fluctuation.[22] Because respiratory arrhythmia is a common event in dogs[29], measurements obtained with the DPD method versus other methods are suggested to be more accurate in that species.

Intraobserver within- and between-day and interobserver repeatability for RTX_{PD} measurement were low in the present study. This is in disagreement with the results of a previous study[23], in which between-day CV for RTX_{PD} in 55 healthy dogs was 15.3%. This difference may be related to the number of measurements, in that 3 cardiac cycles were used in the present study versus 20 cycles in the other study.

High intraobserver and low interobserver repeatability of RTX_{TD} measurement were obtained in the present study. To date, repeatability of RTX_{TD} measurement in dogs

has lacked adequate evaluation. For humans, high[30–32] and low[33] repeatability of RTX_{TD} measurement have been reported. The RTX_{TD} can also be measured in a single cardiac cycle; therefore, it is not influenced by heart rate fluctuations. Low interobserver repeatability in humans and the dogs of the present study may be attributable in part to that fact that limits of the different intervals for tissue Doppler echocardiography are often poorly defined and may be too sensitive to the mild changes, such as hemodynamic shifts or slight differences in the obtained images.[33]

The RTX_{TD} values were higher than the RTX_{DPD} and RTX_{PD} values of the dogs of the present study. This finding was consistent with findings of previous studies involving humans[30,31] and dogs[21]. The higher RTX_{TD} was mainly attributable to the longer interval between tricuspid valve closure and opening and isovolumic time derived from the tissue Doppler method, compared with values obtained with DPD and pulsed-wave Doppler methods. The reason for differences between RTX_{TD} and other RTX measurements may have been related to differences in methods used and measurement site.[22,31] The RTX_{TD} is measured by use of intervals based on myocardial motion, whereas the RTX_{DPD} and RTX_{PD} are measured by use of intervals based on blood flow.[31] Moreover, RTX_{TD} is measured only at the right ventricular inlet portion, in contrast to RTX_{DPD} and RTX_{PD}, which are measured at both the right ventricular inlet and outlet portion; therefore,

RTX_{TD} may be unrelated to the overall right ventricular function.[22,31] It is important to consider that RTX_{TD} had higher reference values than RTX_{DPD} and RTX_{PD}; therefore, RTX should not be used interchangeably.

In humans with RV pressure-overload, RTX_{DPD} is a better predictor of exercise capacity than RTX_{TD} and RTX_{PD}.[22] Therefore, in dogs with RV pressure-overload, as occurs with PH, RTX_{DPD} may also be a better predictor of right heart dysfunction. Additional studies are needed to validate the clinical usefulness of RTX_{DPD} in dogs with right heart dysfunction.

The present study had several limitations. First, a small number of healthy laboratory Beagles was used; therefore, caution has to be exercised in extrapolating these repeatability data to dogs with right heart dysfunction. Indeed, in humans, the degree of disagreement among RTX values in patients with heart disease is higher than that in healthy subjects.[32] Second, no reference standard of the RV function, such as cardiac catheterization, was evaluated in the present study. Therefore, we could not assess which of the 3 methods for RTX measurement was superior. Additional studies are needed to validate the correlation between RTX and the RV function obtained by cardiac catheterization and other noninvasive echocardiographic indices, such as TAPSE or FAC. Third, DPD echocardiography is a novel application of ultrasonography that is available

on only few ultrasonography systems, so the usefulness of RTX_{DPD} measurement may be limited in clinical settings.

The study reported here revealed that RTX_{DPD} measurement was feasible and reliable method for evaluation of cardiac function in a small number of healthy dogs. The RTX_{DPD} values were not significantly different from the RTX_{PD} values; however, RTX_{TD} values were significantly higher than RTX_{DPD} and RTX_{PD} values. Therefore, RTX values derived from different methods should be interpreted with caution and not used interchangeably because the values differ with each method. Investigations involving dogs with heart disease are warranted to determine the clinical applicability of RTX_{DPD} measurement.

5. SUMMARY

In this chapter, the repeatability of the RTX measurements and the degrees of agreement RTX values derived from 3 different echocardiographic methods in healthy dogs have established. RTX_{DPD} measurement had high within-day and interobserver repeatability, and RTX_{TD} measurement had high within-day repeatability. In addition, the RTX_{TD} values were significantly higher than the RTX_{DPD} and RTX_{PD} values. Therefore, RTX values derived from different echocardiographic methods should be interpreted with caution.

CHAPTER 2

THE REPEATABILITY AND CHARACTERISTICS OF RIGHT VENTRICULAR LONGITUDINAL STRAIN IMAGING BY SPECKLE TRACKING ECHOCARDIOGRAPHY IN HEALTHY DOGS

1. INTRODUCTION

STE is a novel quantitative method for assessment of the regional and global myocardial deformation from greyscale B-mode images. In humans, STE has been applied to analysis of RV function, and demonstrated to be a feasible and sensitive quantitative technique.[34] RVLS has been shown to correlate well with invasive hemodynamic variables, and impaired RVLS has been strongly predicted to lead to a poor outcome in human patients with PH and advanced systolic heart failure.[35–40] In addition, RV-SD6 has been demonstrated to be a good predictor of a reduced cardiac function, clinical worsening, and poor prognosis in human patients with PH.[41–43]

Few reports are available on RVLS measurement derived from STE in dogs. High repeatability and the reference intervals of free wall and septal RVLS, and the correlation between these values and body weight have been reported in healthy dogs.[16,17] However, the RVLS values using different ultrasound systems and offline software have been reported to be different in human medicine.[44–46] In addition, RV-SD6 has not been evaluated in these reports.

Thus, the goal of chapter 2 was to elucidate the repeatability of the RVLS and RV-SD6 measurement derived from STE in healthy dogs, and to validate the effects of

the body weight, heart rate, age, and sex on echocardiographic indices of RV function, including RVLS and RV-SD6 in clinically healthy dogs with different body weights.

2. MATERIALS AND METHODS

2.1 Dogs

Five laboratory Beagles (one female, four males; 2-4 years; 9.5-13.0 kg) were used for assessing repeatability in this study. All dogs were determined to be healthy and have a normal heart anatomy and myocardial function based on normal findings on complete physical examination, electrocardiography, and standard echocardiographic examinations (including B-mode, M-mode, pulsed-wave Doppler, and color flow Doppler imaging).

Client-owned dogs referred to the Veterinary Teaching Hospital of Hokkaido University with no cardiovascular disorder between December 2013 and April 2016, and 14 laboratory Beagles formed the clinically healthy dog group. The owner`s consent for each dog was obtained before its enrollment in this study. Exclusion criteria included the presence of a heart murmur, pathologic arrhythmia, and a history of heart or respiratory disease. All dogs were determined to have a normal heart anatomy and myocardial function based on normal findings on complete physical examination, electrocardiography, and standard echocardiographic examinations (including B-mode, M-mode, pulsed-wave Doppler, and color flow Doppler imaging). Arterial blood

pressures were measured indirectly by means of the oscillometric method (PetMAP graphic; Ramsey Medical Inc., Tampa, FL, USA). Trivial tricuspid and pulmonic regurgitation evident on color flow Doppler imaging was defined as physiologic "silent regurgitation" if silent to auscultation and associated with a normal valve morphology. Dogs with "silent regurgitation" across the tricuspid and pulmonic valve were not excluded because this is considered physiologic in many healthy dogs.[47] The most common reasons for ultrasonographic evaluations of client-owned dogs were preanesthetic evaluation for magnetic resonance imaging (73 dogs) and health assessment (30 dogs). Dogs were recruited based on their body weight and were classified into 4 groups: very small (≤ 4 kg); small (4.1 to 8 kg); medium (8.1 to 20 kg); large (>20 kg).

All procedures were approved by the Laboratory Animal Experimentation Committee, Graduate School of Veterinary Medicine, Hokkaido University (Approval No. 15-0087).

2.2 Echocardiographic measurements

All echocardiographic measurements were performed using commercially available ultrasound equipment (Artida; Toshiba Medical Systems Corporation, Tochigi, Japan) equipped with a 3 to 6 MHz sector probe (PST-50BT; Toshiba Medical Systems Corporation, Tochigi, Japan). All dogs were examined while manually restrained in left

and right lateral recumbent positions without sedation. An ECG trace (lead II) was recorded simultaneously with echocardiographic imaging and an automatically measured heart rate. S'_{TV} was determined by tissue Doppler at the lateral tricuspid annulus with an apical 4-chamber view (Figure 3). TAPSE was obtained by placing an M-mode cursor over the tricuspid annulus with an apical 4-chamber view and measuring its amplitude of motion during systole (Figure 3). The RV end-diastolic area (RVEDA) and end-systolic area (RVESA) were obtained by tracing the RV endocardium in systole and diastole from the annulus to apex with the modified apical four chamber view, which included the RV apex, and then the FAC was calculated as (RVEDA − RVESA)/RVEDA × 100% (Figure 3). The RTX was calculated by tissue Doppler method as shown chapter 1 (Figure 3).

2.3 Right ventricular longitudinal strain and RV-SD6 analysis by speckle tracking echocardiography

RVLS and RV-SD6 measurement were performed using conventional grayscale echocardiography with a modified apical four-chamber view. The frame rate was optimized to >200 frames/s by narrowing the imaging sector and reducing the depth to focus on the RV. Three consecutive cardiac cycles were stored on a hard drive, and the images were analyzed using offline software (2D Wall Motion Tracking; Toshiba Medical Systems Corporation, Tochigi, Japan). The value for STE indices was determined from

the average of three cardiac cycles. Care was taken to obtain the best visualization of the RV endocardial border from the base to apex. The endocardial border was manually traced in an end-diastolic frame, and the region of interest was generated followed by adjustments to incorporate the entire RV wall myocardial thickness. The RV wall was divided into inner and outer layers, and the RV free wall and septal wall were divided into three segments (basal, middle, and apical), respectively. RVLS is defined as the percentage shortening of a region of interest relative to its original length, and is expressed as a negative percentage during systole.[48] RVLS was obtained for each segment at the highest peak of the software-generated strain curves of the inner layer. Global RVLS was calculated by averaging values observed in all six segments of the RV, and free wall RVLS and septal RVLS were calculated by averaging each value of three segments along the entire RV (Figure 4). SST was calculated from the QRS onset to maximum peak longitudinal strain of each of the RV 6segments of the RV. To quantify RV intraventricular dyssynchrony, RV-SD6 was calculated as the SD of the SST of RV 6segments using offline software (2D Wall Motion Tracking; Toshiba Medical Systems Corporation, Tochigi, Japan) (Figure 4), and RV-SD6 was corrected for the RR interval according to Bazett's formula: Corrected RV-SD6 = RV-SD6/$\sqrt{\ }$RR interval.[49]

2.4 Statistical analysis

Power calculations for sample size determination were made on the basis of data from previous study[24]. Presuming a similar intraobserver within-day, intraobserver between-day, and interobserver intraclass correlation coefficient (ICC), it was estimated that a sample size of 5 dogs would be required in this study to provide a power of 80% to demonstrate ICC = 0.75[24], a null hypothesis of ICC = 0, with $\alpha = 0.05$, and the numbers of measurement is 3 times.[25] Statistical analyses were performed using computer software (JMP version 8.0 and SPSS version 21; SPSS Inc., Chicago, IL, USA). The normal distribution of the data was confirmed by means of a Shapiro-Wilk test.

The following linear model was used for the variables in within- and between-day and interobserver variability analysis[26]:

$$Y_{ijkl} = \mu + \text{Observer}_i + \text{Day}_j + \text{Dog}_k + (\text{Observer} \times \text{Dog})_{ik} + (\text{Day} \times \text{Dog})_{jk} + \varepsilon_{ijkl}$$

where Y_{ijkl} was the first value measured for dog k on day j by observer i, μ was the general mean, Observer_i was the differential effect (considered as fixed) of observer i, Dog_k was the differential effect of dog k, $(\text{Observer} \times \text{Dog})_{ik}$ is the interaction term between the observer and dog, (Day × Dog) is the interaction term between day and dog, and ε_{ijkl} is the model error. The SD of within-day variability was estimated as the residual

SD of the model, SD of between-day variability as the SD of the differential effect of day, and SD of interobserver variability as the SD of the differential effect of observer. The CV were determined by dividing each SD by the mean.

The intraobserver within-day ICC was determined from data generated by the same observer; this echocardiographer evaluated 5 dogs 3 times repeatedly during the same day. The intraobserver between-day ICC was determined from data generated by 1 observer; on 3 different days, this echocardiographer made 3 evaluations of the 5 dogs. The interobserver ICC was determined from data generated by 2 blinded observers on the same day; these echocardiographers evaluated 5 dogs 3 times repeatedly during the same day. Agreement was considered marked when CV < 20%[26,27], ICC was reported as indicating poor to very good agreement: < 0.2 is considered as poor agreement, 0.21-0.40 as fair agreement, 0.41-0.60 as moderate agreement, 0.61-0.80 as good agreement, 0.81-1.0 as very good agreement.[34]

The correlation between echocardiographic indices and characteristics (body weight, age, and heart rate) were evaluated by Pearson`s correlation coefficient test. In multiple linear regression analysis with forward stepwise selection, Akaike information criteria were used to assess the relationships between echocardiographic indices and characteristics (body weight, age, sex, and heart rate). Differences between males and

females regarding echocardiographic indices of RV function were evaluated with an unpaired *t*-test. The significance of differences between the different body weight groups was evaluated by ANOVA. If ANOVA was significant, Tukey HSD test was used as a post-hoc test. Values of $P < 0.05$ were considered significant. Data are shown as the mean ± SD.

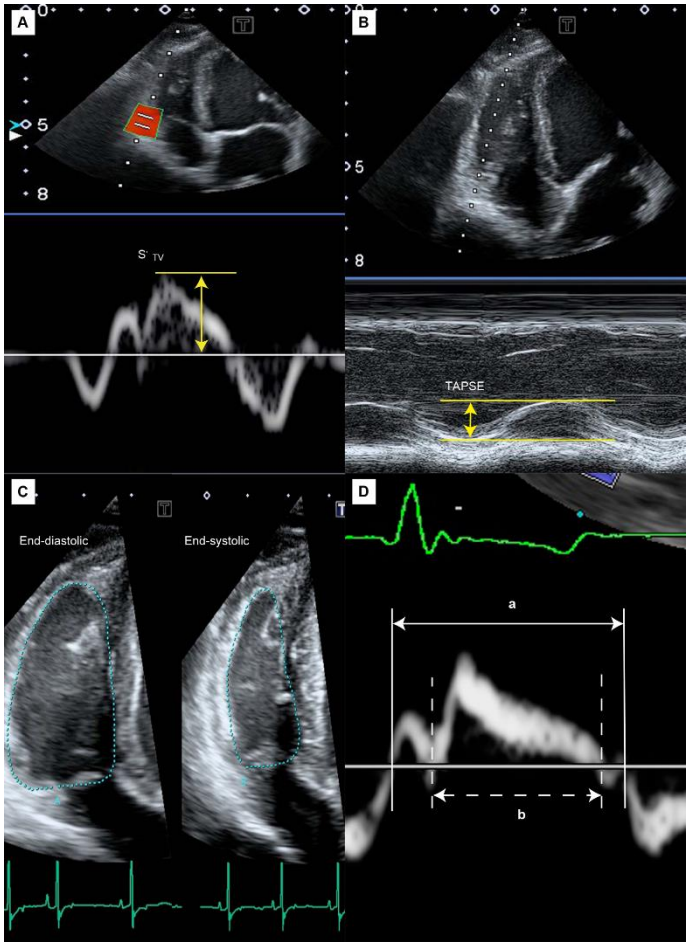

Figure 3. Echocardiographic images illustrating a technique used to measure the echocardiographic indices of RV function. A－S'_{TV} was determined by measuring the maximum velocity during systole using tissue Doppler at the lateral tricuspid annulus with an apical 4-chamber view. B－TAPSE was determined by measuring its amplitude of tricuspid annulus motion during systole using the M-mode with an apical 4-chamber view. C－FAC was calculated with a modified apical 4-chamber view as follows: (RV end-diastolic area – RV end-systolic area)/RV end-diastolic area × 100%. D－RTX was calculated with a left parasternal short-axis view using tissue Doppler as follows: (a –

b)/b. FAC, fractional area change; RV, right ventricle; S'_{TV}, peak systolic tricuspid annular velocity; TAPSE, tricuspid annulus plane systolic excursion.

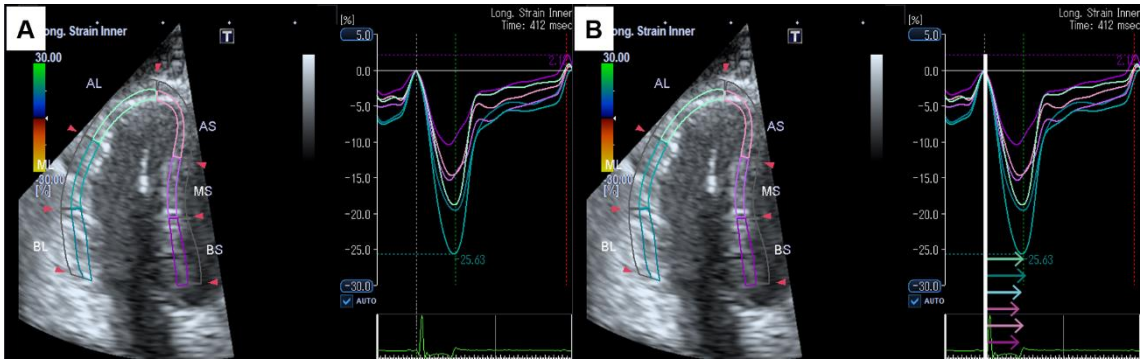

Figure 4. Echocardiographic images illustrating a technique used to measure RVLS and RV-SD6. RV free wall and septum were automatically divided into 3 segments (apical, middle, and basal), respectively. A－Global RVLS was calculated by averaging the peak longitudinal strain values in all 6 segments of the RV with a modified apical 4-chamber view, B－RV-SD6 was calculated as the standard deviation of the systolic shortening time of the 6 RV segments, and corrected for the R-R interval (Bazett's formula). The colored arrows indicate each segmental systolic shortening time. AL, apical lateral free wall; AS, apical septum; BL, basal lateral free wall; BS, basal septum, ML, middle lateral free wall; MS, middle lateral septum. RV, right ventricle; RVLS, right ventricular longitudinal strain; RV-SD6, standard deviation of the time to systolic shortening time of right ventricular 6segments.

3. RESULTS

Repeatability of RVLS and RV-SD6

Global, free wall, septal RVLS, and RV-SD were determined for all obtained images (90 cardiac cycles of 5 Beagles). Intraobserver within- and between-day and interobserver CVs and ICCs of global, free wall, septal RVLS, and RV-SD6 are summarized in Table 3. Intraobserver within-day repeatability of RVLS and RV-SD were very good (ICC of > 0.80). Intraobserver between-day repeatability of RVLS was moderate to good (ICC of 0.58-0.78), and interobserver repeatability of RVLS was good (ICC of 0.70-0.80). In contrast, intraobserver between-day repeatability of RV-SD6 was moderate (ICC of 0.45), and interobserver repeatability of RV-SD6 was fair (ICC of 0.21).

Reference values and comparison between different body weight groups

Data were collected from 14 Beagles and 103 privately owned dogs. These dogs belonged to 30 different breeds, with Chihuahua being the most frequently represented (n = 17,14.5%), followed by Miniature dachshund (n = 15, 12.7%), Beagle (n = 14, 12.0%), Miniature poodle (n = 10, 8.5%), mixed breeds (n = 8, 6.8%). The data on characteristics and echocardiographic indices of RV function of the breeds represented by the highest number of dogs (Chihuahua, Miniature dachshund, Beagle, and Miniature poodle) are

summarized in Table 4. Thirty-two dogs were classified into the very small dog group, 36 were classified into the small dog group, 32 were classified into the medium dog group, and 17 were classified into the large dog group. Mild physiologic tricuspid regurgitation was observed in 17 of the 117 dogs (14.5%). The data on characteristics and echocardiographic indices of RV function in the 4 groups are summarized in Table 5. Free wall RVLS was higher than septal RVLS (19.0 ± 3.1 vs. 15.3 ± 2.7, respectively, $P <$ 0.0001).

Global, free wall, and septal RVLS in large dogs were significantly lower compared with those in the other groups. The RV-SD6 in large dogs was significantly higher than the other groups. Values for S'_{TV} and TAPSE in medium and large dogs were significantly higher than in very small and small dogs. The RTX in large dogs was significantly higher than in very small dogs. FAC in medium and large dogs was significantly lower than in very small and small dogs.

Correlation analysis between echocardiographic indices and characteristics

The correlations between the echocardiographic indices of RV function and body weight, heart rate, and age are summarized in Table 6. Global, free wall, and septal RVLS were negatively correlated with the body weight, and RV-SD6 was positively correlated with the body weight. In addition, S'_{TV}, TAPSE, and the RTX were positively correlated

with the body weight, and FAC was negatively correlated with the body weight. While there was no correlation with STE indices and the age, S'_{TV} and TAPSE were negatively correlated with the age. There was no significant difference between male and female dogs regarding the echocardiographic indices of RV function.

Multiple linear regression analysis between echocardiographic indices and characteristics

All echocardiographic indices of RV function (STE and conventional indices) were significantly correlated with the body weight. Furthermore, TAPSE was significantly correlated with the age. In contrast, there was no correlation with the sex.

Table 3. Within-day, between-day, and interobserver repeatability for measurements of speckle tracking echocardiographic indices in five healthy Beagles.

Variable	Within-day		Between-day		Interobserver	
	CV (%)	ICC	CV (%)	ICC	CV (%)	ICC
Global RVLS	3.4	0.90	12.7	0.78	5.2	0.80
Free wall RVLS	5.3	0.91	4.4	0.77	6.6	0.79
Septal RVLS	5.9	0.85	10.8	0.58	7.1	0.70
RV-SD6	13.3	0.84	29.2	0.45	51.7	0.21

CV, coefficients of variation; ICC, intraclass correlation coefficient; RVLS, right ventricular longitudinal strain; RV-SD6, standard deviation of the systolic shortening time of right ventricular 6segments corrected for the RR interval according to Bazett's formula.

Table 4. Characteristics and the values of echocardiographic indices in 56 dogs of 4 different breeds.

	Chihuahua	Miniature dachshund	Beagle	Miniature poodle
Number of dogs	17	15	14	10
Male/Female	11/6	9/6	8/6	5/5
Age (years)	6.3 ± 2.8	8.1 ± 3.0	1.4 ± 0.9	6.4 ± 2.8
Body weight (kg)	3.0 ± 1.2	5.0 ± 1.4	11.3 ± 1.1	4.4 ± 1.1
Heart rate (bpm)	114 ± 25	88 ± 24	110 ± 21	93 ± 29
Mean blood pressure (mmHg)	109 ± 10	107 ± 21	109 ± 8	116 ± 16
Global RVLS × - 1 (%)	16.6 ± 2.0	17.6 ± 1.8	17.3 ± 2.1	19.3 ± 3.2
Free wall RVLS × - 1 (%)	18.5 ± 3.0	19.9 ± 1.9	18.9 ± 2.5	21.2 ± 4.0
Septal RVLS × - 1 (%)	14.6 ± 2.1	15.7 ± 2.3	16.0 ± 2.2	17.4 ± 3.5
RV-SD6 (msec)	12.0 ± 5.5	-11.8 ± 4.5	16.1 ± 7.6	13.7 ± 3.8
S'_{TV} (cm/sec)	11.0 ± 3.1	9.9 ± 2.4	13.8 ± 3.7	10.4 ± 2.3
TAPSE (mm)	8.5 ± 2.0	9.1 ± 1.8	14.5 ± 2.0	9.4 ± 3.1
FAC (%)	46.9 ± 5.5	42.7 ± 7.1	36.7 ± 5.0	45.5 ± 1.9
RTX	0.49 ± 0.06	-0.53 ± 0.04	0.53 ± 0.06	0.50 ± 0.03

Data are presented as mean ± SD.

FAC, fractional area change; RTX, right ventricular Tei index; S'_{TV}, peak systolic tricuspid annular velocity; TAPSE, tricuspid annulus plane systolic excursion.

See Table 3 for remainder of key.

Table 5. Characteristics and the values of echocardiographic indices in 117 clinically healthy dogs.

	All dogs	Very small*	Small*	Medium*	Large*
Number of dogs	117	32	36	32	17
Male/Female	64/53	17/15	21/15	17/15	9/8
Age (years)	6.0 ± 3.6	6.5 ± 3.1 [a]	6.8 ± 3.3 [a]	5.4 ± 3.9 [a]	4.7 ± 4.3 [a]
Body weight (kg)	9.6 ± 8.8	2.7 ± 0.8 [a]	5.3 ± 1.1 [b]	11.4 ± 2.3 [c]	28.0 ± 6.7 [d]
Heart rate (bpm)	100 ± 24	106 ± 26 [a]	95 ± 27 [a]	102 ± 22 [a]	97 ± 15 [a]
Mean blood pressure (mmHg)	109 ± 15	113 ± 15 [a]	109 ± 15 [a]	108 ± 12 [a]	102 ± 17 [a]
Global RVLS × - 1 (%)	17.1 ± 2.5	17.6 ± 2.3 [a]	17.9 ± 2.3 [a]	17.3 ± 2.0 [a]	14.5 ± 2.4 [b]
Free wall RVLS × - 1 (%)	19.0 ± 3.1	19.7 ± 2.9 [a]	19.9 ± 2.8 [a]	19.0 ± 2.6 [a]	15.8 ± 2.9 [b]
Septal RVLS × - 1 (%)	15.3 ± 2.7	15.6 ± 2.6 [a]	15.7 ± 2.8 [a]	15.7 ± 2.0 [a]	13.1 ± 2.9 [b]
RV-SD6 (msec)	13.8 ± 6.5	-11.9 ± 5.7 [a]	12.9 ± 5.1 [a]	12.9 ± 6.7 [a]	19.3 ± 6.9 [b]
S'_{TV} (cm/sec)	11.6 ± 3.4	-10.1 ± 3.3 [a]	10.5 ± 2.3 [a]	12.8 ± 3.4 [b]	14.6 ± 2.9 [b]
TAPSE (mm)	10.9 ± 3.1	-8.1 ± 2.0 [a]	9.9 ± 2.0 [b]	13.0 ± 2.4 [c]	13.9 ± 2.9 [c]
FAC (%)	41.5 ± 8.0	-45.1 ± 6.3 [a]	44.1 ± 6.9 [a]	38.3 ± 6.8 [b]	35.1 ± 9.3 [b]
RTX	0.52 ± 0.05	-0.50 ± 0.05 [a]	0.51 ± 0.05 [ab]	0.53 ± 0.05 [ab]	0.54 ± 0.07 [b]

Data are presented as mean ± SD.

See Tables 3 and 4 for key.

[a, b]Values in the same row with different superscript letters are significantly ($P < 0.05$; Tukey HSD) different.

* Very small, Body weight of ≤ 4 kg; Small, Body weight of 4.1 to 8 kg; Medium, Body weight of 8.1 to 20 kg, Large, Body weight of > 20 kg.

Table 6. Correlation analysis of echocardiographic indices and characteristics in 117 clinically healthy dogs.

	Body weight	Heart rate	Age
Global RVLS	- 0.46*	- 0.14	- 0.02*
Free wall RVLS	- 0.46*	- 0.07	- 0.09*
Septal RVLS	- 0.32*	- 0.16	- 0.05*
RV-SD6	- 0.35*	- 0.14	- 0.13*
S'_{TV}	- 0.48*	- 0.15	- 0.24*
TAPSE	- 0.62*	- 0.01	- 0.32*
FAC	- 0.42*	- 0.10	- 0.01*
RTX	- 0.31*	- 0.23	- 0.06*

The numbers represent the correlation coefficients (r).

See Tables 3 and 4 for key.

* $P < 0.05$.

4. DISCUSSION

The major findings of our study are the following: (1) repeatability of RVLS and RV-SD6 by STE was high with the exception of between-day and interobserver repeatability of RV-SD6; (2) free wall RVLS was higher than septal RVLS; (3) in large dogs (BW > 20 kg), all RVLS values were significantly lower, and RV-SD6 was significantly higher than in smaller dogs; (4) all RVLS and FAC were negatively, and RV-SD6, S'_{TV}, TAPSE, and RTX were positively, correlated with the body weight; (5) all echocardiographic indices of RV function were significantly related to the body weight on multiple regression analysis.

The repeatability of RVLS was high (ICC of > 0.60), except for between-day septal RVLS (ICC of 0.58) in the present study. This finding agrees with previous reports on humans and dogs.[16,17,34] Therefore, the measurement of RVLS by STE is clinically feasible. While within-day repeatability of RV-SD6 was high (ICC of 0.84), between-day and interobserver repeatability of RV-SD6 were low (ICC of 0.45 and 0.21, respectively). Similar findings have been reported in humans and dogs.[44,50] In these previous studies, between-day and interobserver repeatability of SD of the time to the peak longitudinal strain of the LV in healthy humans[44] and SD of the time to peak radial strain of LV in

dogs with mitral valvular disease[50] were low. The low repeatability of RV-SD6 may be partly explained by the relatively low frame rate to the heart rate. In the present study, the frame rate was optimized to > 200 frames/s; however, the frame rate might not be sufficient to quantify intraventricular dyssynchrony. It is important for RV-SD6 to be interpreted with careful consideration of the between-day and interobserver repeatability.

In the present study, free wall RVLS was higher than septal RVLS in healthy dogs. This result is in line with a previous study on healthy humans and dogs.[17,51] In human patients with PH, both free wall RVLS and septal RVLS have been shown to be decreased compared with healthy humans[36,37,51], and to significantly correlate with the pulmonary arterial pressure[36]. While impaired free wall RVLS has been reported to strongly predict a poor outcome in patients with PH and advanced systolic heart failure[38–40], the utility of septal RVLS as a predictor of a poor outcome has not been clarified. However, in the present study, both free wall RVLS and septal RVLS were measured, because the RV systolic function may depend on the contraction of not only the free wall but also septum. Indeed, only septal RVLS was found to be significantly lower in human patients with acute pulmonary embolism than in healthy controls[52], and the septal RVLS was preserved as a compensatory mechanism for impaired free wall RVLS in patients with right heart disease.[53]

In addition, free wall RVLS in the present study were lower than those in a previous study on health dogs[16,17] (free wall RVLS, 19.0 ± 3.2 vs. 28.6 ± 4.0 or 24.9 ± 6.1). The reason for the difference may be related to ultrasound systems and offline analysis software from different vendors. In the present study, Artida and 2D Wall Motion Tracking (Toshiba Medical Systems) was used for STE, and Vivid 7 and EchoPac (GE Medical Systems) or MyLab 50 and XStrain™ (Esaote) was used in the previous study. The longitudinal strain values of the LV using Artida have been reported to be lower than those using GE and Esaote in healthy humans.[44–46] Several factors, such as a different tracking algorithm, analytical software, and region of interest, may contribute to this difference.[44–46]

The large dogs (BW > 20 kg) had significantly lower RVLS values and higher RV-SD6 values than smaller dogs (BW ≤ 20 kg) in the present study. Our results support the previously reported findings in healthy dogs.[54] In the previous study, LV radial and circumferential strain were significantly decreased, and the dyssynchrony index (difference in the time to peak strain from the earliest to latest segment of the LV) was significantly increased in large dogs (BW > 20 kg).[54] One possible reason for the lower STE values in large dogs is a less synchronized manner of RV contraction in the longitudinal direction. Although the specific mechanism is still unknown, the time

required for the propagation of RV systole may be prolonged because of the large size of the heart in larger dogs.

In the present study, RVLS, RV-SD6, and conventional indices (S'_{TV}, TAPSE, FAC, and the RTX) were significantly correlated with the body weight. Furthermore, multiple linear regression analysis revealed that all echocardiographic indices of the RV function were significantly related to the body weight. In previous studies, conventional indices of RV function, including S'_{TV}, TAPSE, FAC and RVLS, were shown to be correlated with the body weight in healthy dogs.[16,17] Our findings agree with the previous reports on dogs. To our knowledge, the present study provides the first description of the effects of the body weight on RV-SD6 in dogs. In the present study, RV-SD6 was significantly related to body weight; therefore, the body weight should be taken into consideration when evaluating RV dyssynchrony by STE in a clinical setting.

The RTX was significantly correlated with the body weight in the present study. Our findings conflict with previous studies on healthy dogs.[13,23] The reason for this difference in effects of the body weight on the RTX may be related to the number of dogs and difference in method. The number of dogs in these previous studies was smaller than in our study (n = 53 and 45 vs. 117, respectively). Moreover, in the previous studies, pulsed-wave Doppler echocardiography was used to measure the RTX, in contrast to our

study using tissue Doppler echocardiography. We previously reported that the RTX measured with different methods should not be used interchangeably.[55]

S'_{TV} and TAPSE were negatively correlated with the age. This finding supports a previous human study.[56] Our findings indicate that the body weight and age should be taken into consideration when we evaluate the cardiac function by echocardiography in a clinical setting.

There remain several limitations in the present study. First, only a small number of healthy laboratory Beagles was evaluated for repeatability analysis. Therefore, caution has to be exercised on extrapolating these repeatability data to dogs with right heart dysfunction. Second, the possibility that the dogs used as healthy dogs had subclinical cardiac disease cannot be excluded. Third, a dog breed effect on echocardiographic indices of the RV function may be present, because various dog breeds with a small number of dogs as healthy dogs was included in this study. Further studies using a larger number of dogs should be performed to clarify whether there is a breed effect on echocardiographic indices of the RV function in dogs. Fourth, only the RV longitudinal strain, and not radial or circumferential strain was performed. Because of complex geometry, the assessments of RV radial and circumferential strains are difficult. The modality of 3D-echocardiography may be able to assess various direction strains. Fifth,

the reference values showed in this study should only be applied when using the same echocardiography device with the same offline software, because the values using different methods can change. Sixth, the RV strain was measured using software for the LV strain, because RV-specific strain analysis software has yet to be developed. Finally, image quality affects the repeatability of STE measurement and different image quality may therefore affect future results.

In conclusion, RV longitudinal strain imaging by STE was a feasible method in healthy dogs. Speckle tracking and conventional echocardiographic indices of RV function were affected by the body weight and age. Therefore, evaluation of the cardiac function based on echocardiographic indices of RV function should be interpreted with caution in a clinical setting.

5. SUMMARY

In this chapter, the repeatability of the RVLS and RV-SD6 measurements have established in healthy Beagles. In addition, the relationship between echocardiographic indices of RV function and characteristics (body weight, heart rate, blood pressure, and sex) have validated in clinically healthy dogs.

RVLS had high within-day, between-day, and interobserver repeatability. While RV-SD6 had high within-day repeatability, between-day and interobserver repeatability were low. All echocardiographic indices of RV function and dyssynchrony were related to body weight, and S'_{TV} and TAPSE were related to age. Therefore, evaluation of cardiac function based on these echocardiographic indices of RV function should be interpreted with caution in a clinical setting.

CHAPTER 3

CHANGES IN RIGHT VENTRICULAR FUNCTION ASSESSED BY ECHOCARDIOGRAPHY IN DOG MODELS OF RV PRESSURE-OVERLOAD

1. INTRODUCTION

PH is a progressive and life-threatening disease characterized by increased in pulmonary vascular resistance (PVR) and pulmonary arterial pressure (PAP), leading to RV pressure-overload, RV dysfunction, and ultimately death. PH is defined as an increase in mean PAP of ≥ 25 mmHg at rest by right heart catheterization (RHC).[57] RV hemodynamic deterioration measured by RHC, such as increased PAP and PVR, and decreased CI, has been associated with poor clinical outcome in human patients with PH.[1,2,58–60]

In clinical practice, RHC is invasive, expensive, and time-consuming for serial assessment. In contrast, echocardiography is the most useful screening tool to diagnose PH and to assess the severity of PH. To our knowledge, no reports are available on the relationship between invasive hemodynamic variables obtained by RHC and the echocardiographic indices of RV function and dyssynchrony in dogs. Thus, the goal of chapter 3 was to elucidate the effects of RV pressure-overload on echocardiographic indices of RV function and dyssynchrony.

2. MATERIALS AND METHODS

2.1 Dogs

Seven laboratory Beagles (3 females and 4 males; 2-4 years; 9.1-12.5 kg) were used in this study. All dogs were determined to be healthy and have a normal heart anatomy and myocardial function based on normal findings on complete physical examination, electrocardiography, and standard echocardiographic examinations. All procedures were approved by the Laboratory Animal Experimentation Committee, Graduate School of Veterinary Medicine, Hokkaido University. (Approval No. 15-0087).

2.2 Study protocol

The dogs were sedated with atropine sulfate (0.05 mg/kg, SC, Atropine Sulfate Injection, Mitsubishi Tanabe Pharma Corp., Osaka, Japan), butorphanol tartrate (0.2 mg/kg, IV, Vetorphale, Meiji Seika Pharma Co. Ltd., Tokyo, Japan), and midazolam hydrochloride (0.1 mg/kg, IV, Dormicum Injection, Astellas Pharma Inc., Tokyo, Japan). Then, the dogs were administered heparin sodium (100 IU/kg, IV, Heparin Sodium Injection, Ajinomoto Pharmaceuticals Co. Ltd., Tokyo, Japan) and cefazolin sodium hydrate (20 mg/kg, IV, Cefamezin α, Astellas Pharma Inc., Tokyo, Japan). The dogs were then anesthetized with propofol (6 mg/kg, IV, Propofol Mylan, Mylan Inc., Canonsburg,

PA, USA.) and intubated. Anesthesia was maintained using a mixture of 1.5-2.0% isoflurane (Isoflu, DS Pharma Animal Health Co. Ltd., Osaka, Japan) and 100% oxygen. The end-tidal partial pressure of carbon dioxide was monitored and maintained between 35 and 45 mmHg by mechanical ventilation. The tidal volume was 10-15 mL/kg and the respiratory rate was maintained at 10-12 breaths/min. The heart rate and arterial blood pressure (BP) via arterial catheterization were monitored and recorded using a polygraph instrument (RMC-4000; Nihon Kohden, Tokyo, Japan). Lactated Ringer's solution (Solulact, Terumo Corp., Tokyo, Japan) was infused at rates of 7 mL/kg/hr via the cephalic vein.

Following a stabilization period of about 10 min, baseline recordings of hemodynamic variables and echocardiographic indices were performed. After baseline measurement, U46619 (9,11-dideoxy-11α,9α-epoxymethanoprostaglandin F2α; Sigma-Aldrich, Saint Louis, MO, USA.) at 50 μg/mL diluted with normal saline was continuous infused via the cephalic vein. U46619 is a thromboxane A2 analog, and intravenous infusion of U46619 induces pulmonary arterial constriction in dogs.[61] Continuous intravenous infusion of U46619 was started at 0.3 μg/kg/min, and titrated at rates of 0.6 and 0.9 μg/kg/min. The infusion rate was determined based on a previous study[61] and the results of our preliminary study. At 15 min after continuous intravenous infusion of

U46619, hemodynamic variables were measured, and then echocardiography was performed. Following the examinations, the dogs were allowed to recover from anesthesia.

2.3 Hemodynamic measurements

All hemodynamic variables were recorded by a polygraph instrument. The anesthetized dogs were positioned in left lateral recumbency. A 6-Fr introducer sheath (FAST-CATH Hemostasis Introducers, St. Jude Medical, Minnetonka, MN, USA.) was percutaneously inserted through the right jugular vein, and then a 5-Fr Swan-Ganz catheter (Swan-Ganz thermodilution catheter, Edwards Lifesciences, Irvine, CA, USA.) was inserted and advanced into the PA under fluoroscopic guidance. The systolic, mean, and diastolic PAP, mean right ventricular pressure (RVP), mean central venous pressure (CVP), and mean pulmonary artery wedge pressure (PAWP) were measured and calculated as the average of 5 consecutive cardiac cycles. The cardiac output (CO) was measured by the thermodilution technique and calculated as the average of 4 measurements. The CI was calculated by dividing the CO by the body surface area. The first derivatives of the maximum RVP change (max dP/dt) and the time constant of RV relaxation (Tau) were calculated from the RVP data. The PVR and systemic vascular resistance (SVR), and PVR to SVR ratio (Rp/Rs) were derived as follows.

PVR = (mean PAP – mean PAWP)/CO, SVR = (mean BP – mean CVP)/CO

Rp/Rs = PVR/SVR.

2.4 Echocardiographic measurements

Echocardiographic measurements were performed using Artida and HI VISION Preirus. The echocardiographic equipment used in this chapter was as described in chapter 1 and 2. HI VISION Preirus was used to measure the RTX by DPD. An ECG trace (lead II) was recorded simultaneously with echocardiographic imaging and automatically measured heart rate.

As detailed in chapter 2, echocardiographic indices of RV function (S'_{TV}, TAPSE, FAC, and RTX) were measured. RVLS and RV-SD6 measurement by STE are as detailed in chapter 2.

2.5 Statistical analysis

Statistical analyses were performed using computer software (JMP version 10.0 and SPSS version 21). Normal distribution of the data was confirmed by a Shapiro-Wilk test. A linear mixed model was developed with dose (baseline, 0.3, 0.6, and 0.9 μg/kg/min) as a categorical fixed effect, and dog identity as a random effect. The *F* test was performed to assess the effect of dose on the values of the measured variables. Pairwise comparisons between the baseline and each dose were performed by obtaining

the least square means and using the Bonferroni correction to account for multiple comparisons. Partial correlation analysis controlling for the effect of dogs was used to determine the relationship between hemodynamic variables and echocardiographic indices. Partial correlation analysis was developed with echocardiographic indices as an outcome variable, and hemodynamic variables as an explanatory variable. Dog was treated as a categorical factor using a dummy variable with 6 degrees of freedom. Multiple linear regression analysis with forward stepwise selection and Akaike information criteria were used to determine the independent predictive value of mean PAP, PVR, CI and Tau. Candidate predictors were S'_{TV}, TAPSE, FAC, RTX, free wall RVLS, septal RVLS, RV-SD6.

Values of $P < 0.05$ were considered significant.

3. RESULTS

Changes in hemodynamic variables

Hemodynamic variable changes before (baseline) and after continuous intravenous infusion of U46619 are summarized in Table 7 and Figure 5 (A and B). Mean BP, systolic PAP, diastolic PAP, mean PAP, mean RVP, PVR, and SVR were significantly higher than baseline at infusion rates of 0.6 and 0.9 μg/kg/min. Mean CVP and Tau were significantly higher than baseline at infusion rates of 0.3, 0.6, and 0.9 μg/kg/min. Rp/Rs was significantly higher than baseline at an infusion rate of 0.6 μg/kg/min. Mean PAWP was significantly higher than baseline at an infusion rate of 0.9 μg/kg/min. In contrast, CI was significantly lower than baseline at infusion rates of 0.6 and 0.9 μg/kg/min. Max dP/dt did not change with continuous intravenous infusion of U46619.

Changes in echocardiographic indices

Changes in echocardiographic indices at baseline and after continuous intravenous infusion of U46619 are summarized in Table 8 and Figure 5 (C-F). An example of baseline and after infusion of U46619 at infusion rates of 0.9 μg/kg/min is shown in Figure 6. FAC was significantly decreased, and RTX was significantly increased at infusion rates of 0.6 and 0.9 μg/kg/min. S'_{TV} and TAPSE were significantly decreased

at an infusion rate of 0.9 μg/kg/min. Free wall and global RVLS were significantly decreased at infusion rates of 0.6 and 0.9 μg/kg/min. In contrast, septal RVLS did not change with continuous intravenous infusion of U46619. Figure 7 shows segmental RVLS and SST at baseline and after continuous intravenous infusion of U46619. Basal and middle free wall RVLS were significantly decreased at infusion rates of 0.6 and 0.9 μg/kg/min, in contrast to apical free wall, basal septal, middle septal, and apical septal RVLS. Free wall SST was significantly longer than baseline at an infusion rate of 0.9 μg/kg/min. Basal free wall SST was significantly longer than baseline at an infusion rate of 0.6 and 0.9 μg/kg/min. RV-SD6 was significantly increased at an infusion rate of 0.9 μg/kg/min. There was a slightly high septal to free wall systolic delay at an infusion rate of 0.9 μg/kg/min, but this was not significant ($P = 0.21$).

Partial correlation analysis between echocardiographic indices and hemodynamic variables

Partial correlations controlling for the effect of dogs between echocardiographic indices and hemodynamic variables are summarized in Table 9. There were significant correlations between PVR, CI and all echocardiographic indices. There were significant correlations between mean PAP and echocardiographic indices except for septal RVLS. However, there were no significant correlations among RVEDA, QRS duration, and

echocardiographic indices.

Multiple linear regression analysis

Multiple linear regression analysis revealed that free wall RVLS and RV-SD were an independent predictor of the mean PAP (free wall RVLS, β = -0.60, $P < 0.001$; RV-SD6, β = 0.40, $P = 0.011$, Table 10). Free wall RVLS, RV-SD6, and RTX were an independent predictor of PVR (free wall RVLS, β = -0.39, $P = 0.020$; RV-SD6, β = 0.47, $P = 0.0086$; RTX, β = 0.34, $P = 0.047$, Table 10). In addition, RTX and S'_{TV} were an independent predictor of CI (RTX, β = -0.65, $P < 0.001$; S'_{TV}, β = 0.35, $P = 0.0030$, Table 10). RTX was an independent predictor of Tau (β = 0.39, $P = 0.0017$, Table 10).

Table 7. Least square means (95% confidence intervals) obtained from the linear mixed model for ECG and hemodynamic variables baseline and after continuous intravenous infusion of U46619 in dog models of RV pressure-overload.

	Baseline	U46619		
		0.3 μg/kg/min	0.6 μg/kg/min	0.9 μg/kg/min
QRS duration (msec)	58 (56-60)	58 (56-60)	59 (57-61)	58 (56-60)
Heart rate (beat/min)	108 (98-118)	99 (89-109)	97 (87-107)	103 (93-113)
Mean BP (mmHg)	54 (48-60)	63 (55-71)	68 (60-76)*	83 (75-91)*
Systolic PAP (mmHg)	13 (11-15)	14 (12-17)	19 (16-21)*	22 (19-24)*
Mean PAP (mmHg)	10 (8-13)	12 (10-15)	17 (14-19)*	19 (17-22)*
Diastolic PAP (mmHg)	8 (6-10)	10 (8-13)	15 (13-17)*	17 (15-19)*
Mean RVP (mmHg)	6 (4-7)	7 (6-9)	9 (8-11)*	10 (9-12)*
Mean CVP (mmHg)	1 (0-2)	2 (1-3)*	3 (2-4)*	3 (2-4)*
Mean PAWP (mmHg)	5 (3-7)	5 (3-7)	6 (4-8)	8 (6-9)*
CI (L/min/m^2)	4.5 (3.9-5.1)	4.4 (3.8-5.0)	3.6 (3.0-4.2)*	3.0 (2.4-3.6)*
Max dP/dt (mmHg/sec)	90 (76-104)	85 (71-99)	90 (76-104)	99 (85-113)
Tau (msec)	135 (81-189)	180 (126-234)*	204 (150-258)*	208 (154-262)*
PVR (WU)	2.5 (1.5-3.5)	3.5 (2.5-4.5)	6.2 (5.2-7.2) *	8.1 (7.1-9.1)*
SVR (WU)	24.0 (16.2-31.8)	28.2 (20.4-36.0)	37.8 (30.0-45.6)*	56.8 (49.0-64.6)*
Rp/Rs	0.11 (0.09-0.13)	0.12 (0.10-0.14)	0.17 (0.15-0.19)*	0.15 (0.13-0.17)

BP, blood pressure; CI, cardiac index; CVP, central venous pressure; Max dP/dt, maximum positive rate of RV pressure change; PAP, pulmonary arterial pressure; PAWP, pulmonary artery wedge pressure; PVR, pulmonary vascular resistance; Rp/Rs, PVR to SVR ratio; RVP, right ventricular pressure; SVR, systemic vascular resistance; Tau, time constant of RV relaxation.

* $P < 0.05$ compared with the baseline.

Table 8. Least square means (95% confidence intervals) obtained from the linear mixed model for echocardiographic indices baseline and after continuous intravenous infusion of U46619 in dog models of RV pressure-overload.

	Baseline	U46619		
		0.3 μg/kg/min	0.6 μg/kg/min	0.9 μg/kg/min
E (m/sec)	0.43 (0.37-0.49)	0.40 (0.34-0.46)	0.30 (0.24-0.36)*	0.25 (0.19-0.31)*
A (m/sec)	0.37 (0.29-0.45)	0.44 (0.36-0.52)	0.42 (0.34-0.50)*	0.43 (0.35-0.51)*
E/A	1.20 (0.94-1.46)	0.97 (0.71-1.23)	0.81 (0.55-1.07)*	0.62 (0.36-0.88)*
S'_{TV} (cm/sec)	6.9 (5.9-7.9)	6.5 (5.5-7.5)	5.8 (4.8-6.8)	5.1 (4.1-6.1)*
TAPSE (mm)	7.2 (6.6-7.8)	7.7 (7.1-8.3)	6.6 (6.0-7.2)	5.8 (5.2-6.4)*
RVEDA (cm^2)	6.0 (4.6-7.4)	6.9 (5.5-8.3)	6.7 (5.3-8.2)	6.1 (4.6-7.5)
RVESA (cm^2)	4.3 (3.2-5.5)	5.2 (4.0-6.4)	5.4 (4.2-6.5)*	4.9 (3.7-6.1)
FAC (%)	30.4 (26.4-34.4)	26.2 (22.2-30.2)	20.8 (16.8-24.8)*	20.4 (16.4-24.4)*
RTX	0.26 (0.16-0.36)	0.32 (0.22-0.42)	0.45 (0.35-0.55)*	0.63 (0.53-0.73)*
Global RVLS × - 1 (%)	11.8 (9.6-14.0)	12.0 (9.8-14.2)	9.1 (6.9-11.3)*	8.3 (6.1-10.5)*
Free-wall RVLS × - 1 (%)	13.2 (11.2-15.2)	13.0 (10.8-15.2)	9.3 (7.1-11.5)*	8.2 (6.0-10.4)*
Basal free wall	13.8 (10.6-17.0)	11.7 (8.5-14.9)	8.1 (4.9-11.3)*	7.4 (4.2-10.6)*
Middle free wall	13.8 (11.6-16.0)	13.4 (11.2-15.6)	10.5 (8.3-12.7)*	8.9 (6.7-11.1)*
Apical free wall	8.5 (6.1-10.9)	8.1 (5.7-10.5)	7.2 (4.8-9.6)	7.0 (4.6-9.4)
Septal RVLS × - 1 (%)	10.4 (7.6-13.2)	10.9 (8.1-13.7)	9.2 (6.4-12.0)	9.0 (6.2-11.8)
Basal septum	11.4 (8.6-14.2)	11.6 (8.8-14.4)	10.8 (8.0-13.6)	9.2 (6.4-12.0)
Middle septum	9.6 (7.4-11.8)	10.5 (8.3-12.7)	9.2 (7.0-11.4)	8.7 (6.5-10.9)
Apical septum	6.8 (5.0-8.6)	7.0 (5.2-8.8)	5.8 (4.0-7.6)	6.8 (5.0-8.6)
Free wall SST (msec)	261 (215-307)	272 (226-318)	321 (275-367)	345 (299-391)*
Basal free wall	263 (209-317)	272 (219-327)	339 (285-393)*	373 (319-427)*
Middle free wall	261 (221-301)	279 (239-319)	299 (259-339)	303 (263-343)
Apical free wall	262 (220-304)	286 (244-328)	297 (255-339)	313 (271-355)
Septal SST (msec)	257 (205-309)	279 (227-331)	299 (247-351)	310 (258-362)
Basal septum	263 (213-313)	286 (236-336)	301 (251-351)	311 (261-361)
Middle septum	263 (211-315)	280 (228-332)	291 (239-343)	307 (255-359)
Apical septum	260 (208-312)	297 (245-349)	313 (261-365)	318 (266-370)
Septal to free wall	4	-7	22	35

systolic delay (msec)	(- 33-41)	(- 44-30)	(- 15-59)	(- 2-72)
RV-SD6 (msec)	25 (9-41)	24 (8-40)	50 (34-66)	66 (50-82)*

A, tricuspid valve late diastolic flow velocity; E, tricuspid valve early diastolic flow velocity; FAC, fractional area change; RTX, right ventricular Tei index; RVEDA, right ventricular end-diastolic area; RVESA, right ventricular end-systolic area; RVLS, right ventricular longitudinal strain; RV-SD6, standard deviation of the systolic shortening time of right ventricular 6segments corrected for RR interval according to Bazett's formula; SST, systolic shortening time; S'_{TV}, peak systolic tricuspid annular velocity; TAPSE, tricuspid annular plane systolic excursion.

* $P < 0.05$ compared with the baseline.

Table 9. Partial correlation analysis of echocardiographic indices and hemodynamic variables controlling for the effect of dogs in dog models of RV pressure-overload.

	Mean PAP	PVR	CI
S'_{TV}	- 0.44*	- 0.56*	- 0.67*
TAPSE	- 0.47*	- 0.53*	- 0.67*
FAC	- 0.66*	- 0.69*	- 0.54*
RTX	- 0.73*	- 0.83*	- 0.83*
Global RVLS	- 0.75*	- 0.80*	- 0.67*
Free wall RVLS	- 0.78*	- 0.77*	- 0.62*
Septal RVLS	- 0.27*	- 0.40*	- 0.43*
RV-SD6	- 0.79*	- 0.83*	- 0.57*

See Table 7 and 8 for key.

* $P < 0.05$.

Table 10. Multiple linear regression analysis of predictors of the mean PAP, PVR, CI, and Tau in dog models of RV pressure-overload.

Predictor	β	SE	*P* value
Mean PAP *			
RV-SD6	- 0.40	0.02	0.011
Free wall RVLS	- 0.60	0.20	< 0.001
PVR †			
RV-SD6	- 0.47	0.02	0.0086
Free wall RVLS	- 0.39	0.11	0.020
RTX	0.34	2.16	0.047
CI ‡			
RTX	- 0.65	0.45	< 0.001
S'_{TV}	0.35	0.07	0.0030
Tau §			
RTX	0.39	39.6	0.0017

See Table 7 and 8 for key

* Adjusted $R^2 = 0.84$, † Adjusted $R^2 = 0.87$, ‡ Adjusted $R^2 = 0.91$, § Adjusted $R^2 = 0.85$.

β = Standard regression coefficient.

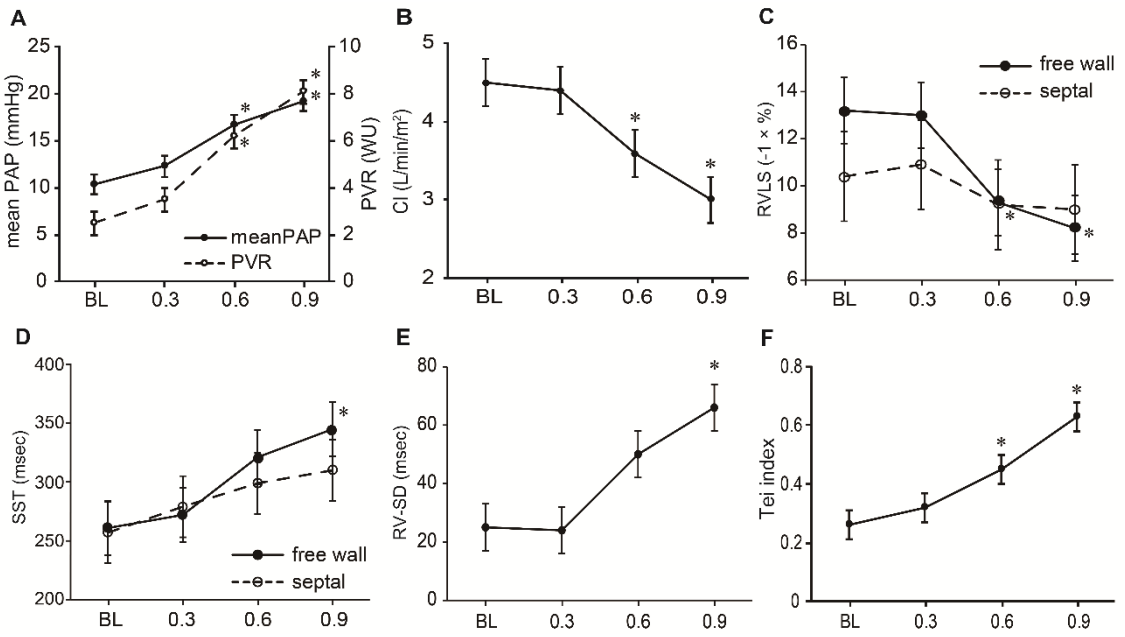

Figure 5. Dose-dependent changes in the hemodynamic variables and echocardiographic indices after U46619 infusion in dog models of RV pressure-overload. Data are shown as the least square means ± SE. A－Mean PAP and PVR. B－CI. C－Free wall and septal RVLS. D－Free wall and septal SST. E－RV-SD6. F－RTX.

* $P < 0.05$ compared with the baseline.

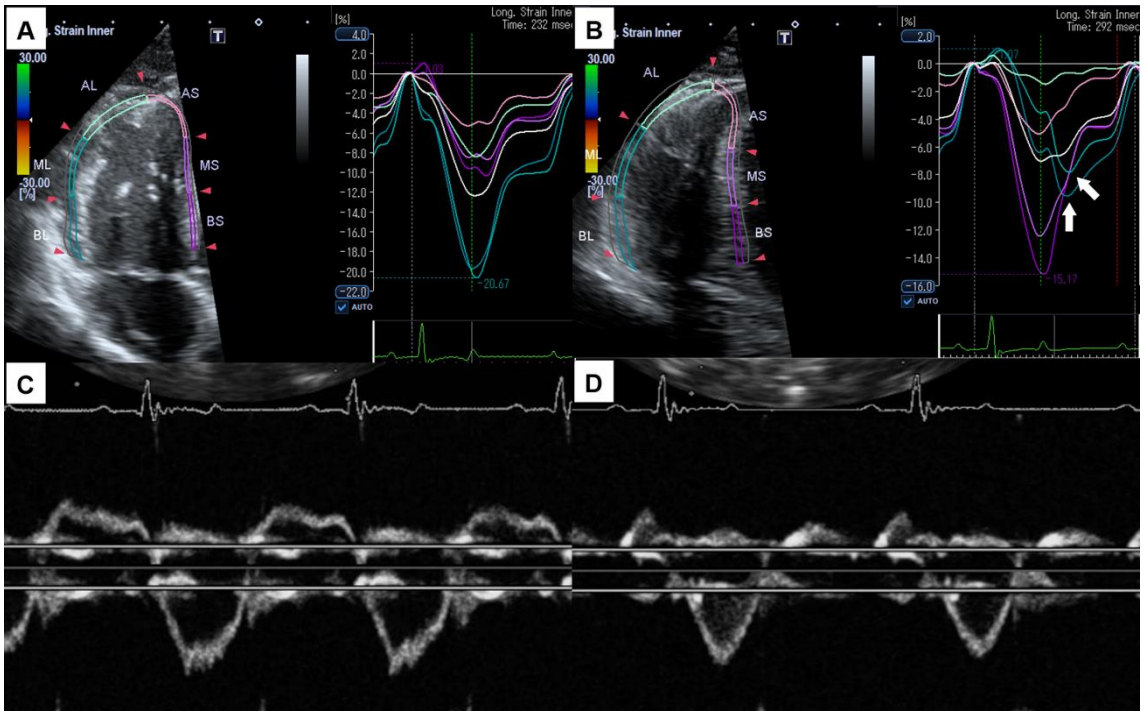

Figure 6. Representative images of speckle tracking echocardiograph and right ventricular Tei index (RTX) at baseline (A, C) and after U46619 infusion (B, D). A－Global right ventricular longitudinal strain (RVLS) was –11.8%, and RV-SD6 was 25 msec at baseline. B－RTX was 0.20 at baseline. C－After U46619 infusion at 0.9 μg/kg/min, global RVLS was decreased (–7.4%). Systolic shortening time of basal and middle free wall was delayed (white arrows), and RV-SD6 was increased (60 msec). D－RTX was increased (0.70) after U46619 infusion at 0.9 μg/kg/min. White color curve indicates global RVLS. RV-SD6, standard deviation of the systolic shortening time of right ventricular 6segments.

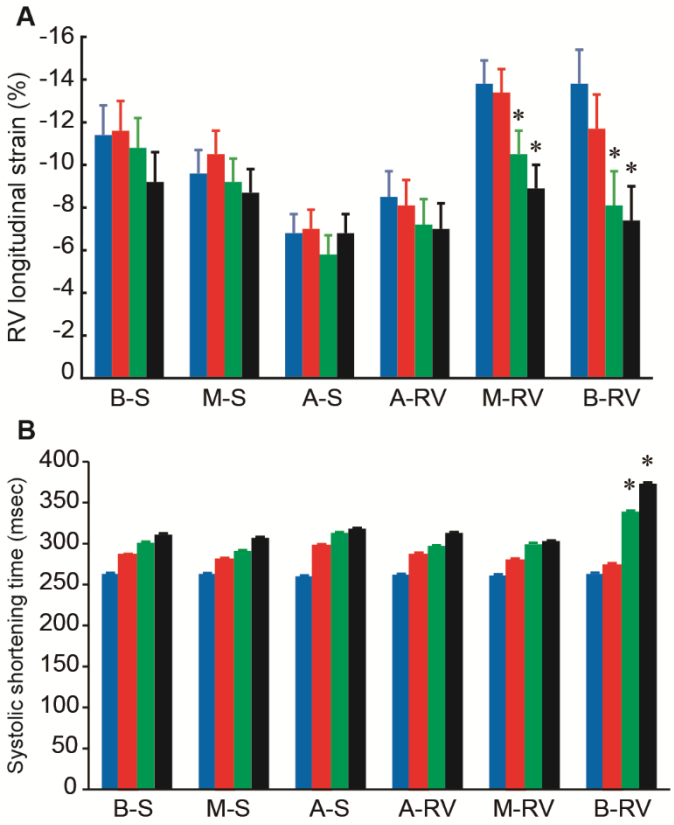

Figure 7. Dose-dependent segmental right ventricular longitudinal strain (RVLS) and systolic shortening time (SST) change after U46619 infusion in dog models of RV pressure-overload. Data are shown as the least square means ± SE. A, Basal and middle free wall RVLS were significantly lower than baseline at infusion rates of 0.6 and 0.9 μg/kg/min. B, Basal free wall SST was significantly longer than baseline at an infusion rate of 0.6 and 0.9 μg/kg/min. Blue bar, baseline; red bar, 0.3μg/kg/min; green bar, 0.6μg/kg/min; black bar, 0.9μg/kg/min. A-RV, apical free wall; A-S, apical septum; B-RV, basal free wall; B-S, basal septum; M-RV, middle free wall; M-S, middle septum. * $P < 0.05$ compared with the baseline.

4. DISCUSSION

The main finding of this study is that echocardiographic indices of RV function, including RVLS and RV-SD derived from STE, are impaired under an RV pressure-overload condition, and were an independent predictor of the mean PAP and PVR. These findings indicate that RVLS and RV-SD6 are sensitive to RV pressure-overload.

In present study, while free wall RVLS significantly decreased and was correlated significantly with the mean PAP and PVR, septal RVLS did not change in dog models of RV pressure-overload. Li et al.[35] and Puwanant et al.[36] have reported that septal RVLS by STE significantly decreased in patients with PH compared with normal controls, and was correlated with PAP. The reason for this difference in septal RVLS may be related to the difference in the severity or duration of RV pressure-overload. In our study, systolic PAP of the dog models of RV pressure-overload was 22 ± 1 mmHg in contrast to a previous study, which included patients with systolic PAP of > 43.0 ± 4.6 mmHg[35] and 71 ± 23 mmHg[36] estimated by echocardiography. Our findings indicate that free wall RVLS has higher sensitivity to RV pressure-overload compared with septal RVLS under an RV pressure-overload condition. The result of free wall RVLS is similar to previous studies in patients with PH.[6,35–38]

Furthermore, basal and middle free wall RVLS were significantly decreased in the present study. In contrast, apical free wall RVLS and all segmental septal RVLS did not change in dog models of RV pressure-overload. McConnell's sign, characterized by severe hypokinesis of the middle and basal RV free wall with a preserved apical RV free wall motion based on subjective wall motion evaluation, is a well-recognized pattern and useful for echocardiographic diagnosis in patients with acute pulmonary embolism.[62] However, patients with McConnell's sign actually had lower apical free wall RVLS compared with those without McConnell's sign, and this sign has been associated with higher PVR, RV dilation, and systolic dysfunction.[63,64] In present study, apical free wall RVLS was preserved after U46619 infusion similar to baseline, therefore the findings of the present study may be a mild impairment in RV wall motion under an RV pressure-overload condition rather than McConnell's sign, and basal and middle free wall may be sensitive to RV pressure-overload.

In the present study, RV-SD6 increased significantly after U46619 infusion, and was significantly correlated with the mean PAP, PVR, and CI. RV intraventricular dyssynchrony has been described in human patients with PH, and has been demonstrated to be a good predictor of reduced cardiac function, such as RV ejection fraction and CI, clinical worsening, and poor prognosis.[5,6,41,42] RV dyssynchrony has been reported to be

caused by RV pressure-overload, chamber dilation, and electrical activation delay.[5,6,41,42,65] In our study, RV-SD6 showed no association with RVEDA and QRS duration. Therefore, RV dyssynchrony may be mainly caused by RV pressure-overload under this condition.

Marcus et al.[5] and Kalogeropoulos et al.[6] reported free wall systolic delay using STE and magnetic resonance imaging in patients with PH. Our study showed that basal free wall SST was longer, and septal to free wall systolic delay was high after U46619 infusion, but was not significant. The reason might be explained by the lesser degree of RV pressure-overload or the small sample size (n = 7) in our study. Indeed, the mean PAP in Kalogeropoulos et al.'s study and Marcus et al.'s study were 45 ± 13 mmHg and 55 ± 13 mmHg, respectively.

RV muscle is mainly composed of longitudinal muscle fibers, and the tricuspid annulus move toward the apex during the systolic phase. Therefore, longitudinal function of RV is essential in determination of RV output.[66] In the present study, conventional RV function indices, such as S'_{TV}, TAPSE, and FAC, were correlated with the mean PAP, PVR, and CI. This is consistent with the findings of previous studies in humans.[67,68] However, in multivariate analysis, these echocardiographic indices were not independent predictors of the mean PAP and PVR. While these conventional RV

function indices have been used in clinical setting and provide information on global RV function, they have some limitations. S'_{TV} and TAPSE can only assess regional analysis of tricuspid annulus and are angle-dependence. The measurement of FAC is experience-dependent and reproducibility is often poor. Our results indicate that the superiority of STE-derived indices and RTX, for assessing hemodynamic deterioration compared with conventional RV function indices under an RV pressure-overload condition.

RTX increased significantly under an RV pressure-overload condition, and was an independent predictor of PVR and CI. This result is in line with previous studies in patients with PH[18,19,65]. Furthermore, diastolic function, as assessed by Tau, was impaired in dog models of RV pressure-overload. These findings indicate that diastolic dysfunction is caused by RV pressure-overload. Similar findings have been reported in the human patients with PH[69], and pig models of PH induced by U46619[70]. In previous studies using a high-fidelity micromanometer[69] or conductance catheter[70], diastolic function, as assessed by Tau, was impaired. Moreover, in our study, RTX was an independent predictor of Tau. Our study findings suggest that RTX reflects not only hemodynamic deterioration, but also diastolic dysfunction caused by RV pressure-overload.

In present study, U46619 infusion significantly elevated not only PVR and PAP, but also the BP, PAWP and SVR in a dose-dependent manner. These hemodynamic

changes may influence the echocardiographic indices of RV function. Indeed, echocardiographic indices of RV systolic and diastolic function by conventional and STE impaired in patients with systemic hypertension without PH.[71,72]

There remain several limitations of the present study. First, as mention above, U46619 infusion significantly elevated not only PVR and PAP, but also the BP, PAWP and SVR in a dose-dependent manner. A previous humans and dogs study showed a similar change of hemodynamic variables.[61,70,73] These results indicate that U46619 induces not only pulmonary arterial constriction, but also systemic arterial constriction. Previous studies demonstrated that U46619 induced pulmonary arterial vasoconstriction[74], and canine isolated coronary, basilar, and mesenteric arteries vasoconstriction[75]. However, in our study, Rp/Rs significantly increased after U46619 infusion, therefore the main target of U46619 may be the PA. Second, in the present study, a Swan-Ganz catheter was used for measuring hemodynamic variables. A high-fidelity micromanometer would have strengthened the results, especially max dP/dt and Tau. Third, while RV systolic function was assessed by max dP/dt in this study, it is load-dependent and does not accurately reflect RV contractility. Therefore, measurement of load-independent indices derived from RV pressure-volume loops using a conductance catheter, such as ventricular end-systolic elastance and effective arterial elastance, is

needed to clarify the relationship between echocardiographic indices and RV systolic function. Fourth, the possibility that general anesthesia may have modulated myocardial performance and echocardiographic indices cannot be excluded. Moreover, a complete autonomic blockade was not used in the present study. Fifth, the number of dogs in this study was small.

In conclusion, echocardiographic indices of RV function, such as free wall RVLS, RV-SD6, and RTX, are useful for assessing hemodynamic changes under an RV pressure-overload condition, compared with conventional echocardiographic indices.

5. SUMMARY

In this chapter, the effects of RV pressure-overload on the echocardiographic indices of RV function in dog models of RV pressure-overload by U46619 infusion were investigated. Compared with baseline values, all echocardiographic indices of RV function and dyssynchrony were impaired after U46619 infusion, and these indices were significantly correlated with the mean PAP, PVR, and CI. In addition, on multiple linear regression analysis, free wall RVLS and RV-SD6 were an independent predictor of the mean PAP and PVR, and RTX was an independent predictor of CI. These results indicate that the echocardiographic indices of RV function and dyssynchrony, such as free wall RVLS, RV-SD6, and RTX, are useful for assessing hemodynamic changes under RV pressure-overload condition.

GENERAL CONCLUSION

The goal of this study was to establish the clinical usefulness of the assessment of RV function by echocardiography in dogs with heart disease. The findings of the present study indicate that RTX derived from DPD, RVLS and RV-SD6 derived from STE are feasible and reliable method for evaluation of RV function, and these echocardiographic indices can be used to assess the severity of RV pressure-overload in dogs. These results allow validation of the relationship between the echocardiographic indices of RV function and the hemodynamic changes observed in clinical dogs with heart disease in the future.

In chapter 1, the repeatability of RTX derived from 3 different echocardiographic method was established in healthy dogs. While the within-day, between-day, and interobserver repeatability of RTX_{DPD} measurement were high, those of RTX_{PD} were low. The within-day repeatability of RTX_{TD} was high. In addition, the RTX_{TD} values were significantly higher than RTX_{DPD} and RTX_{PD} values. Thus, these findings indicate that RTX_{DPD} measurement can be applied for the assessment of RV function in dogs.

In chapter 2, the repeatability of RVLS and RV-SD6 derived from STE was investigated in healthy dogs, and the relationship between echocardiographic indices of

RV function and characteristics in clinically healthy dogs. The within-day, between-day, and interobserver repeatability of RVLS was high. The within-day repeatability of RV-SD6 was high, but the between-day and interobserver repeatability of this index were low. In addition, these echocardiographic indices were significantly related to body weight. Therefore, these data demonstrate that the evaluation of RV function and dyssynchrony based on RVLS and RV-SD6 by STE can be applied in dogs. However, the effect of body weight on echocardiographic indices should be taken into consideration in a clinical setting.

In chapter 3, the effects of RV pressure-overload on echocardiographic indices of RV function were investigated in healthy dogs. Compared with baseline values, all echocardiographic indices of RV function were impaired after U46619 infusion. In addition, these echocardiographic indices were significantly correlated with the mean PAP, PVR, and CI. On multiple linear regression, RVLS and RV-SD6 were an independent predictor of the mean PAP and PVR, and RTX was an independent predictor of the CI. Thus, these results demonstrate that RVLS, RV-SD6, and RTX are useful for assessing hemodynamic changes under an RV pressure-overload condition in dogs.

In order to clarify the role of the echocardiographic indices of RV function in dogs with chronic RV pressure-overload in the future, it is necessary to validate the

relationship between invasive hemodynamic variables obtained by RHC and echocardiographic indices in dog models of chronic RV pressure-overload. Furthermore, long-term follow-up studies that can confirm associations between chronic RV pressure-overload and the changes in the echocardiographic indices of RV function in clinical dogs (e.g.. the dogs with PH) are needed. In addition, to validate the usefulness of these echocardiographic indices to evaluate the treatment response, further studies in clinical dogs with RV pressure-overload and dog models of chronic RV pressure-overload are needed.

In conclusion, the applicability of the echocardiographic indices of RV function in dogs including RTX derived from DPD, RVLS, and RV-SD6 derived from STE were able to be established. Additionally, preliminary findings in healthy dogs regarding the relationships between the echocardiographic indices of RV function and RV pressure-overload can be clarified. The assessment of RV function by echocardiography may be useful to evaluate the severity and prognosis in dogs with heart disease.

JAPANESE SUMMARY（要旨）

Application of the assessment of right ventricular function by echocardiography in dogs with heart disease

（犬心疾患への心エコー図法を用いた右心室機能評価の応用）

心エコー図検査は人や犬において心疾患の診断、重症度評価、予後推定に有用な検査であり必須の検査とされている。これまでは全身に血液を拍出する重要な心腔であり多くの心疾患が発生することから、その主な対象は左心室機能であった。しかしながら近年医学では、右心室機能低下が主に右心室が障害される肺高血圧症患者のみならず、左心室が障害される僧帽弁閉鎖不全症や拡張型心筋症患者においても予後不良因子であることが明らかにされてきており、その評価に注目が集まっている。しかしながら心エコー図検査では、右心室の複雑な構造や収縮機構のため従来左心室に適用されていた心エコー図検査指標を用いて右心室機能を評価することは困難とされてきた。そこで今回これらの制限を受けにくい指標として右室 Tei index および新たな技術である Speckle Tracking 法を用いた右心室機能評価に着目した。

右室 Tei index は収縮能と拡張を合わせた総合的な心機能を評価可能な

心エコー図検査指標であり、人および犬においてその有用性が示されている。しかしながら従来法である pulsed-wave Doppler 法による測定では同一心周期での測定を行うことができず、犬に一般的に存在する呼吸性不整脈の影響を受けて再現性が低下する可能性が指摘されている。また組織ドプラ法による測定は同一心周期における測定は可能であるが、pulsed-wave Doppler による測定値との差異が認められている。そこで同一心周期にて測定可能な Dual pulsed-wave Doppler 法による右室 Tei index 測定に注目した。

Speckle Tracking 法は 1 心周期において心筋の動きを自動的に追跡することにより正確に心筋運動を定量化できる新たな心エコー図手法である。医学においては Speckle tracking 法による右心室機能評価は肺高血圧症患者において侵襲的に評価した血行動態と良好に相関し、予後推定にも有用であることが明らかとなってきている。さらに Speckle tracking 法を用いることで右心室自由壁と心室中隔の収縮のタイミングのずれ「同期障害」を評価することも可能であり、同期障害の発生が肺高血圧症患者の重症化および予後推定に有用であることが示されてきている。

しかしながら、犬においてはこれらの心エコー図検査手法に関する研究は乏しく、基礎的な知見を欠いている。そこで本研究では、Dual pulsed-wave Dopper 法による右室 Tei index 測定および Speckle tracking 法による右心室機能、

同期障害評価の犬心疾患における臨床的有用性を確立するために３段階からなる実験を行った。

第１段階として、３つの異なる方法により算出される右室 Tei index による右心室機能評価の犬への応用可能性を検討した。従来の方法である pulsed-wave Doppler 法および組織ドプラ法による Tei index 測定に加え、新たな技術である Dual pulsed-wave Doppler 法を用いた測定の再現性評価および各測定値の差異について検討した。その結果、Dual pulsed-wave Doppler 法による右室 Tei index 測定は日内・日間・検者間変動係数および級内相関係数が全て２０％以下および０．７５以上であり、検査再現性は犬への臨床応用に適したものであった。一方 pulsed-wave Doppler 法による測定は日内・日間・検者間再現性が低く、組織ドプラ法による測定は日内・日間再現性は良好であるものの検者間再現性は低いという結果であった。また組織ドプラ法による右室 Tei index は他 2 法による右室 Tei index と比較して高値であった。以上の結果から、Dual pulsed-wave Doppler 法を用いた右室 Tei index 測定は犬において応用可能であることが示された。

続いて第２段階として、 Speckle tracking 法による右心室機能および同期障害評価の犬への応用可能性を検討した。 Speckle tracking 法では右心室収縮能評価指標である右室 strain および右心室同期障害指標である RV-SD6 を算出した。これらの指標の再現性および体重、心拍数、年齢および血圧との関連性を検

討した。右室 strain および RV-SD6 はともに良好な日内再現性を有していた。さらに右室 strain は良好な日間および検者間再現性を示したものの、RV-SD6 においては日間および検者間再現性は低かった。またこれらの指標は体重の影響を受けることも明らかとなった。以上の結果より、 Speckle tracking 法による右心室機能および同期障害評価は犬においても臨床応用可能であるものの、体重の影響を受けることを考慮する必要があることが明らかとなった。

次いで第３段階として、心エコー図検査による右心室機能評価指標が急性右心室圧負荷条件下において右心室圧負荷の重症度評価に応用可能かを検討するための基礎的実験として、健常犬を用いて選択的肺動脈収縮薬である U46619 の持続投与による急性右心室圧負荷が右心室機能評価指標へ及ぼす影響を検討した。すべての右心室機能評価指標が急性右室圧負荷により悪化し、心臓カテーテル検査にて測定した平均肺動脈圧、肺血管抵抗および心拍出量と有意に相関した。さらに重回帰分析において右室 strain および RV-SD6 は平均肺動脈圧、肺血管抵抗の、右室 Tei index は心拍出量の、独立した規定因子であることが明らかとなった。これらの結果から、急性右心室圧負荷条件下において右室 strain、RV-SD6 および右室 Tei index が右心室圧負荷の重症度評価に有用であることが示された。

今後明らかにすべき研究課題の１つとして、慢性右心室圧負荷条件下に

おける右心室機能評価指標と血行動態指標の間の因果関係の検討が挙げられる。そのためには、慢性右心室圧負荷モデル犬において右心室機能評価指標と心臓カテーテル検査などで侵襲的に測定した血行動態指標との関連性を検討する実験研究や慢性肺高血圧症症例犬の右心室機能評価指標の経時的変化を観察する追跡研究が必要である。加えて、肺高血圧症症例犬の内科療法の治療効果判定における右心室機能評価の有用性についても明らかにしていきたい。そのためには、肺高血圧症症例犬や慢性右心室圧負荷モデル犬において治療による右心室機能評価指標の変化を経時的に観察していく必要がある。さらには、様々な原因による肺高血圧症症例やモデル犬を用いて右心室機能評価指標の変化の違いを検討することで、原因診断における右心室機能評価の有用性も明らかにしたいと考えている。

最後に、本研究により右心室機能評価指標、特に右室 Tei index、 Speckle tracking 法を用いた右室 strain 解析や右心室同期障害評価（RV-SD6）が犬における右心室圧負荷の重症度評価に有用である可能性が示された。今後、心エコー図検査よる正確な右心室機能評価を通して、犬心疾患のより適切な管理・治療の実現が期待される。

REFERENCES

1. Veerdonk MC Van De, Kind T, Marcus JT, Mauritz GJ, Heymans MW, Bogaard HJ, Boonstra A, Marques KM, Westerhof N, Vonk-Noordegraaf A. Progressive right ventricular dysfunction in patients with pulmonary arterial hypertension responding to therapy. J Am Coll Cardiolgy 58, 2511–9, 2011.
2. Brittain EL, Pugh ME, Wheeler LA, Robbins IM, Loyd JE, Newman JH, Larkin EK, Austin ED, Hemnes AR. Shorter survival in familial versus idiopathic pulmonary arterial hypertension is associated with hemodynamic markers of impaired right ventricular function. Pulm Circ 3, 589–98, 2013.
3. Tourneau TL, Deswarte G, Lamblin N, Foucher-Hossein C, Fayad G, Richardson M, Polge AS, Vannesson C, Topilsky Y, Juthier F, Trochu JN, Enriquez-Sarano M, Bauters C. Right ventricular systolic function in organic mitral regurgitation: impact of biventricular impairment. Circulation 127, 1597–608, 2013.
4. Doesch C, Dierks DM, Haghi D, Schimpf R, Kuschyk J, Suselbeck T, Schoenberg SO, Borggrefe M, Papavassiliu T. Right ventricular dysfunction, late gadolinium enhancement, and female gender predict poor outcome in patients with dilated cardiomyopathy. Int J Cardiol 177, 429–35, 2014.

5. Marcus JT, Gan CT, Zwanenburg JJ, Boonstra A, Allaart CP, Götte MJ, Vonk-Noordegraaf A. Interventricular mechanical asynchrony in pulmonary arterial hypertension: left-to-right delay in peak shortening is related to right ventricular overload and left ventricular underfilling. J Am Coll Cardiol 51, 750–7, 2008.

6. Kalogeropoulos AP, Georgiopoulou V V, Howell S, Pernetz MA, Fisher MR, Lerakis S, Martin RP. Evaluation of right intraventricular dyssynchrony by two-dimensional strain echocardiography in patients with pulmonary arterial hypertension. J Am Soc Echocardiogr 21, 1028–34, 2008.

7. Rudski LG, Lai WW, Afilalo J, Hua L, Handschumacher MD, Chandrasekaran K, Solomon SD, Louie EK, Schiller NB. Guidelines for the echocardiographic assessment of the right heart in adults:A report from the American society of echocardiography. J Am Soc Echocardiogr 23, 685–713, 2010.

8. Lang RM, Badano LP, Mor-Avi V, Afilalo J, Armstrong A, Ernande L, Flachskampf FA, Foster E, Goldstein SA, Kuznetsova T, Lancellotti P, Muraru D, Picard MH, Rietzschel ER, Rudski L, et al. Recommendations for cardiac chamber quantification by echocardiography in adults: An update from the American society of echocardiography and the European association of cardiovascular imaging. J Am Soc Echocardiogr 28, 1–39, 2015.

9. Serres F, Chetboul V, Gouni V, Tissier R, Sampedrano CC, Pouchelon JL. Diagnostic value of echo-Doppler and tissue Doppler imaging in dogs with pulmonary arterial hypertension. J Vet Intern Med 21, 1280–9, 2007.

10. Toaldo MB, Poser H, Menciotti G, Battaia S, Contiero B, Cipone M, Diana A, Mazzotta E, Guglielmini C. Utility of tissue Doppler imaging in the echocardiographic evaluation of left and right ventricular function in dogs with myxomatous mitral valve disease with or without pulmonary hypertension. J Vet Intern Med 30, 697–705, 2016.

11. Tai TC, Huang HP. Echocardiographic assessment of right heart indices in dogs with elevated pulmonary artery pressure associated with chronic respiratory disorders, heartworm disease, and chronic degenerative mitral valvular disease. Vet Med (Praha) 58, 613–20, 2013.

12. Pariaut R, Saelinger C, Strickland KN, Beaufrère H, Reynolds CA, Vila J. Tricuspid annular plane systolic excursion (TAPSE) in dogs: reference values and impact of pulmonary hypertension. J Vet Intern Med 26, 1148–54, 2012.

13. Teshima K, Asano K, Iwanaga K, Koie H, Uechi M, Kato Y, Kutara K, Edamura K, Hasegawa A, Tanaka S. Evaluation of right ventricular Tei index (index of myocardial performance) in healthy dogs and dogs with tricuspid regurgitation. J

Vet Med Sci 68, 1307–13, 2006.

14. Nakamura K, Morita T, Osuga T, Morishita K, Sasaki N, Ohta H, Takiguchi M. Prognostic value of right ventricular Tei Index in dogs with myxomatous mitral valvular heart disease. J Vet Intern Med 30, 69–75, 2016.

15. Tei C, Ling LH, Hodge DO, Bailey KR, Oh JK, Rodeheffer RJ, Tajik AJ, Seward JB. New index of combined systolic and diastolic myocardial performance: a simple and reproducible measure of cardiac function-a study in normals and dilated cardiomyopathy. J Cardiol 26, 357–66, 1995.

16. Visser LC, Scansen BA, Schober KE, Bonagura JD. Echocardiographic assessment of right ventricular systolic function in conscious healthy dogs: repeatability and reference intervals. J Vet Cardiol 17, 83–96, 2015.

17. Locatelli C, Spalla I, Zanaboni AM, Brambilla PG, Bussadori C. Assessment of right ventricular function by feature-tracking echocardiography in conscious healthy dogs. Res Vet Sci 105, 103–10, 2016.

18. Ogihara Y, Yamada N, Dohi K, Matsuda A, Tsuji A, Ota S, Ishikura K, Nakamura M, Ito M. Utility of right ventricular Tei-index for assessing disease severity and determining response to treatment in patients with pulmonary arterial hypertension. J Cardiol 63, 149–53, 2014.

19. Blanchard DG, Malouf PJ, Gurudevan S V., Auger WR, Madani MM, Thistlethwaite P, Waltman TJ, Daniels LB, Raisinghani AB, DeMaria AN. Utility of right ventricular Tei index in the noninvasive evaluation of chronic thromboembolic pulmonary hypertension before and after pulmonary thromboendarterectomy. J Am Coll Cardiol Imaging 2, 143–9, 2009.

20. Hori Y, Kano T, Hoshi F, Higuchi S. Relationship between tissue Doppler-derived RV systolic function and invasive hemodynamic measurements. Am J Physiol Heart Circ Physiol 293, H120-5, 2007.

21. Hori Y, Kunihiro S, Hoshi F, Higuchi S. Comparison of the myocardial performance echocardiography and tissue Doppler imaging. Am J Vet Res 68, 1177–82, 2007.

22. Choi JO, Choi JH, Lee HJ, Noh HJ, Huh J, Kang IS, Lee HJ, Lee SC, Kim DK, Park SW. Dual pulsed-wave Doppler tracing of right ventricular inflow and outflow: single cardiac cycle right ventricular Tei index and evaluation of right ventricular function. Korean Circ J 40, 391–8, 2010.

23. Baumwart RD, Meurs KM, Bonagura JD. Tei index of myocardial performance applied to the right ventricle in normal dogs. J Vet Intern Med 19, 828–32, 2005.

24. Rosner B. Multisample inference. In: Rosner B, ed. Fundamentals of biostatistics.

7th ed. Brooks/Cole, 2010:p.568-571.

25. Walter SD, Eliasziw M, Donner A. Sample size and optimal designs for reliability studies. Stat Med 17, 101–10, 1998.

26. Chetboul V, Athanassiadis N, Concordet D, Nicolle A, Tessier D, Castagnet M, Pouchelon JL, Lefebvre HP. Observer-dependent variability of quantitative clinical endpoints: the example of canine echocardiography. J Vet Pharmacol Ther 27, 49–56, 2004.

27. Simpson KE, Devine BC, Gunn-Moore DA, French AT, Dukes-McEwan J, Koffas H, Moran CM, Corcoran BM. Assessment of the repeatability of feline echocardiography using conventional echocardiography and spectral pulse-wave doppler tissue imaging techniques. Vet Radiol Ultrasound 48, 58–68, 2007.

28. Bland JM, Altman DG. Measuring agreement in method comparison studies. Stat Methods Med Res 8, 135–60, 1999.

29. Matsunaga T, Harada T, Mitsui T, Inokuma M, Hashimoto M, Miyauchi M, Murano H, Shibutani Y. Spectral analysis of circadian rhythms in heart rate variability of dogs. Am J Vet Res 62, 37–42, 2001.

30. Acharya G, Pavlovic M, Ewing L, Nollmann D, Leshko J, Huhta JC. Comparison between pulsed-wave Doppler- and tissue Doppler-derived Tei indices in fetuses

with and without congenital heart disease. Ultrasound Obstet Gynecol 31, 406–11, 2008.

31. Duzenli MA, Ozdemir K, Aygul N, Soylu A, Aygul MU, Gök H. Comparison of myocardial performance index obtained either by conventional echocardiography or tissue Doppler echocardiography in healthy subjects and patients with heart failure. Heart Vessels 24, 8–15, 2009.

32. Kakouros N, Kakouros S, Lekakis J, Rizos I, Cokkinos D. Tissue Doppler imaging of the tricuspid annulus and myocardial performance index in the evaluation of right ventricular involvement in the acute and late phase of a first inferior myocardial infarction. Echocardiography 28, 311–9, 2011.

33. Rojo EC, Rodrigo JL, Pérez de Isla L, Almería C, Gonzalo N, Aubele A, Cinza R, Zamorano J, Macaya C. Disagreement between tissue Doppler imaging and conventional pulsed wave Doppler in the measurement of myocardial performance index. Eur J Echocardiogr 7, 356–64, 2006.

34. Oxborough D, George K, Birch KM. Intraobserver reliability of two-dimensional ultrasound derived strain imaging in the assessment of the left ventricle, right ventricle, and left atrium of healthy human hearts. Echocardiography 29, 793–802, 2012.

35. Li Y, Xie M, Wang X, Lu Q, Fu M. Right ventricular regional and global systolic function is diminished in patients with pulmonary arterial hypertension: a 2-dimensional ultrasound speckle tracking echocardiography study. Int J Cardiovasc Imaging 29, 545–51, 2013.

36. Puwanant S, Park M, Popovic ZB, Tang WH, Farha S, George D, Sharp J, Puntawangkoon J, Loyd JE, Erzurum SC, Thomas JD. Ventricular geometry, strain, and rotational mechanics in pulmonary hypertension. Circulation 121, 259–66, 2010.

37. Fukuda Y, Tanaka H, Sugiyama D, Ryo K, Onishi T, Fukuya H, Nogami M, Ohno Y, Emoto N, Kawai H, Hirata K. Utility of right ventricular free wall speckle-tracking strain for evaluation of right ventricular performance in patients with pulmonary hypertension. J Am Soc Echocardiogr 24, 1101–8, 2011.

38. Fine NM, Chen L, Bastiansen PM, Frantz RP, Pellikka PA, Oh JK, Kane GC. Outcome prediction by quantitative right ventricular function assessment in 575 subjects evaluated for pulmonary hypertension. Circ Cardiovasc Imaging 6, 711–21, 2013.

39. Motoji Y, Tanaka H, Fukuda Y, Ryo K, Emoto N, Kawai H, Hirata K. Efficacy of right ventricular free-wall longitudinal speckle-tracking strain for predicting

long-term outcome in patients with pulmonary hypertension. Circ J 77, 756–63, 2013.

40. Cameli M, Righini FM, Lisi M, Bennati E, Navarri R, Lunghetti S, Padeletti M, Cameli P, Tsioulpas C, Bernazzali S, Maccherini M, Sani G, Henein M, Mondillo S. Comparison of right versus left ventricular strain analysis as a predictor of outcome in patients with systolic heart failure referred for heart transplantation. Am J Cardiol 112, 1778–84, 2013.

41. Badagliacca R, Reali M, Poscia R, Pezzuto B, Papa S, Mezzapesa M, Nocioni M, Valli G, Giannetta E, Sciomer S, Iacoboni C, Fedele F, Vizza CD. Right intraventricular dyssynchrony in idiopathic, heritable, and anorexigen-induced pulmonary arterial hypertension: clinical impact and reversibility. J Am Coll Cardiol Imaging 8, 642–52, 2015.

42. Badagliacca R, Poscia R, Pezzuto B, Papa S, Gambardella C, Francone M, Mezzapesa M, Nocioni M, Nona A, Rosati R, Sciomer S, Fedele F, Dario Vizza C. Right ventricular dyssynchrony in idiopathic pulmonary arterial hypertension: determinants and impact on pump function. J Heart Lung Transplant 34, 381–9, 2015.

43. Murata M, Tsugu T, Kawakami T, Kataoka M, Minakata Y, Endo J, Tsuruta H,

Itabashi Y, Maekawa Y, Fukuda K. Right ventricular dyssynchrony predicts clinical outcomes in patients with pulmonary hypertension. Int J Cardiol 228, 912–8, 2017.

44. Takigiku K, Takeuchi M, Izumi C, Yuda S, Sakata K, Ohte N, Tanabe K, Nakatani S. Normal range of left ventricular 2-dimensional strain-Japanesed ultrasound speckle tracking of the left ventricle (JUSTICE) study. Circ J 76, 2623–32, 2012.

45. Nagata Y, Takeuchi M, Mizukoshi K, Wu VC, Lin FC, Negishi K, Nakatani S, Otsuji Y. Intervendor variability of two-dimensional strain using vendor-specific and vendor-independent software. J Am Soc Echocardiogr 28, 630–41, 2015.

46. Farsalinos KE, Daraban AM, Ünlü S, Thomas JD, Badano LP, Voigt JU. Head-to-head comparison of global longitudinal strain measurements among nine different vendors: the EACVI/ASE inter-vendor comparison study. J Am Soc Echocardiogr 28, 1171–81, 2015.

47. Bonagura JD, Miller MW. Doppler Echocardiography II. Color Doppler imaging. Vet Clin North Am Small Anim Pract 28, 1361–89, 1998.

48. Reisner SA, Lysyansky P, Agmon Y, Mutlak D, Lessick J, Friedman Z. Global longitudinal strain: a novel index of left ventricular systolic function. J Am Soc

Echocardiogr 17, 630–3, 2004.

49. Bazett HC. An analysis of the time-relations of electrocardiograms. Heart 7, 353–70, 1920.

50. Zois NE, Tidholm A, Nägga KM, Moesgaard SG, Rasmussen CE, Falk T, Häggström J, Pedersen HD, Åblad B, Nilsen HY, Olsen LH. Radial and longitudinal strain and strain rate assessed by speckle-tracking echocardiography in dogs with myxomatous mitral valve disease. J Vet Intern Med 26, 1309–19, 2012.

51. Meris A, Faletra F, Conca C, Klersy C, Regoli F, Klimusina J, Penco M, Pasotti E, Pedrazzini GB, Moccetti T, Auricchio A. Timing and magnitude of regional right ventricular function: a speckle tracking-derived strain study of normal subjects and patients with right ventricular dysfunction. J Am Soc Echocardiogr 23, 823–31, 2010.

52. Stergiopoulos K, Bahrainy S, Strachan P, Kort S. Right ventricular strain rate predicts clinical outcome in patients with acute pulmonary embolism. Acute Card Care 13, 181–8, 2011.

53. Solarz DE, Witt SA, Glascock BJ, Jones FD, Khoury PR, Kimball TR. Right ventricular strain rate and strain analysis in patients with repaired tetralogy of

Fallot: possible interventricular septal compensation. J Am Soc Echocardiogr 17, 338–44, 2004.

54. Takano H, Fujii Y, Ishikawa R, Aoki T, Wakao Y. Comparison of left ventricular contraction profiles among small, medium, and large dogs by use of two-dimensional speckle-tracking echocardiography. Am J Vet Res 71, 421–7, 2009.

55. Morita T, Nakamura K, Osuga T, Lim SY, Yokoyama N, Morishita K, Ohta H, Takiguchi M. Repeatability and reproducibility of right ventricular Tei index derived from 3 echocardiographic methods for evaluation of cardiac function in dogs. Am J Vet Res 77, 715–20, 2016.

56. Innelli P, Esposito R, Olibet M, Nistri S, Galderisi M. The impact of ageing on right ventricular longitudinal function in healthy subjects: a pulsed tissue Doppler study. Eur J Echocardiogr 10, 491–8, 2009.

57. Galiè N, Humbert M, Vachiery J-L, Gibbs S, Lang I, Torbicki A, Simonneau G, Peacock A, Vonk Noordegraaf A, Beghetti M, Ghofrani A, Gomez Sanchez MA, Hansmann G, Klepetko W, Lancellotti P, et al. 2015 ESC/ERS Guidelines for the diagnosis and treatment of pulmonary hypertension. Eur Heart J 37, 67–119, 2016.

58. Miller WL, Grill DE, Borlaug BA. Clinical features, hemodynamics, and

outcomes of pulmonary hypertension due to chronic heart failure with reduced ejection fraction: Pulmonary hypertension and heart failure. J Am Coll Cardiol Hear Fail 1, 290–9, 2013.

59. Okada O, Tanabe N, Yasuda J, Yoshida Y, Katoh K, Yamamoto T, Kuriyama T. Prediction of life expectancy in patients with primary pulmonary hypertension. A retrospective nationwide survey from 1980-1990. Intern Med 38, 12–6, 1999.

60. Ogawa A, Ejiri K, Matsubara H. Long-term patient survival with idiopathic/heritable pulmonary arterial hypertension treated at a single center in Japan. Life Sci 118, 414–9, 2014.

61. Hori Y, Kondo C, Matsui M, Yamagishi M, Okano S, Chikazawa S, Kanai K, Hoshi F, Itoh N. Effect of the phosphodiesterase type 5 inhibitor tadalafil on pulmonary hemodynamics in a canine model of pulmonary hypertension. Vet J 202, 334–9, 2014.

62. McConnell M V., Solomon SD, Rayan ME, Come PC, Goldhaber SZ, Lee RT. Regional right ventricular dysfunction detected by echocardiography in acute pulmonary embolism. Am J Cardiol 78, 469–73, 1996.

63. Platz E, Hassanein AH, Shah A, Goldhaber SZ, Solomon SD. Regional right ventricular strain pattern in patients with acute pulmonary embolism.

Echocardiography 29, 464–70, 2012.

64. Wright L, Dwyer N, Power J, Kritharides L, Celermajer D, Marwick TH. Right ventricular systolic function responses to acute and chronic pulmonary hypertension: assessment with myocardial deformation. J Am Soc Echocardiogr 29, 259–66, 2016.

65. Ichikawa K, Dohi K, Sugiura E, Sugimoto T, Takamura T, Ogihara Y, Nakajima H, Onishi K, Yamada N, Nakamura M, Nobori T, Ito M. Ventricular function and dyssynchrony quantified by speckle-tracking echocardiography in patients with acute and chronic right ventricular pressure overload. J Am Soc Echocardiogr 26, 483–92, 2013.

66. Haddad F, Hunt SA, Rosenthal DN, Murphy DJ. Right ventricular function in cardiovascular disease, part I: Anatomy, physiology, aging, and functional assessment of the right ventricle. Circulation 117, 1436–48, 2008.

67. Yang T, Liang Y, Zhang Y, Gu Q, Chen G, Ni XH, Lv XZ, Liu ZH, Xiong CM, He JG. Echocardiographic parameters in patients with pulmonary arterial hypertension: correlations with right ventricular ejection fraction derived from cardiac magnetic resonance and hemodynamics. PLoS One 8, e71276, 2013.

68. Forfia PR, Fisher MR, Mathai SC, Housten-Harris T, Hemnes AR, Borlaug BA,

Chamera E, Corretti MC, Champion HC, Abraham TP, Girgis RE, Hassoun PM. Tricuspid annular displacement predicts survival in pulmonary hypertension. Am J Respir Crit Care Med 174, 1034–41, 2006.

69. Murch SD, Gerche AL, Roberts TJ, Prior DL, Andrew I, Burns AT, Murch SD, Gerche A La, Roberts TJ, Prior DL, Macisaac AI, Burns AT. Abnormal right ventricular relaxation in pulmonary hypertension. Pulm Circ 5, 370–5, 2015.

70. Amà R, Leather HA, Segers P, Vandermeersch E, Wouters PF. Acute pulmonary hypertension causes depression of left ventricular contractility and relaxation. Eur J Anaesthesiol 23, 824–31, 2006.

71. Tumuklu MM, Erkorkmaz U, Öcal A. The impact of hypertension and hypertension-related left ventricle hypertrophy on right ventricle function. Echocardiography 24, 374–84, 2007.

72. Pedrinelli R, Canale ML, Giannini C, Talini E, Dell'Omo G, Bello V Di. Abnormal right ventricular mechanics in early systemic hypertension: A two-dimensional strain imaging study. Eur J Echocardiogr 11, 738–42, 2010.

73. Leather HA, Segers P, Berends N, Vandermeersch E, Wouters PF. Effects of vasopressin on right ventricular function in an experimental model of acute pulmonary hypertension. Crit Care Med 30, 2548–52, 2002.

74. Stephenson AH, Sprague RS, Lonigro AJ. 5, 6-Epoxyeicosatrienoic acid reduces increases in pulmonary vascular resistance in the dog. Am J Psysiology 275, H100-109, 1998.

75. Matsuzaki T, Noguchi K, Nakasone J, Uezu K, Higuchi M, Sakanashi M. Effects of the new thromboxane A2 antagonist vapiprost in isolated canine blood vessels. Arzneimittelforschung 42, 1318–22, 1992.

ACKNOWLEDGEMENTS

This PhD study is not one that can be achieved alone. I would like to thank all people who have supported and encouraged me.

First and foremost, I would like to express my gratitude to my supervisor, Dr. Mitsuyoshi Takiguchi (Graduate School of Veterinary Medicine, Hokkaido University) for giving me the opportunities to achieve my goals and aspirations, and for his constant encouragement, support, advice, and guidance.

I wish to also thank Drs. Mutsumi Inaba (Graduate School of Veterinary Medicine, Hokkaido University), and Hiroshi Ohta (Graduate School of Veterinary Medicine, Hokkaido University) for their time and effort to provide advice and critical comments in making this dissertation a better one.

I am also greatly indebted to my mentor, Dr. Kensuke Nakamura (Organization for promotion of Tenure Track, University of Miyazaki) for his time and effort in evaluating my research, presentations, and papers, and for encouragement and guidance.

My gratitude also extends to Drs. Masahiro Yamasaki (Faculty of Agriculture, Iwate University), Keitaro Morishita (Graduate School of Veterinary Medicine, Hokkaido University), Noboru Sasaki (Graduate School of Veterinary Medicine, Hokkaido

University), Takaharu Itami (Graduate School of Veterinary Medicine, Hokkaido University), Tomohito Ishizuka (Graduate School of Veterinary Medicine, Hokkaido University), Kiwamu Hanazono (Graduate School of Veterinary Medicine, Hokkaido University), and Tatsuyuki Osuga (Graduate School of Veterinary Medicine, Hokkaido University) for their constant support and assistance. I also wish to thank my fellow comrades; Drs. Kazuyoshi Sasaoka, Sei Kawamoto, Shogo Ikeda, Shingo Miki, and Nozomu Yokoyama for their priceless advice and support. In addition, I am also thankful to all members of the Laboratory of Veterinary Internal Medicine of Hokkaido University for helping me with my experiments.

I also wish to thank all sweet dogs in my laboratory for contributions to my PhD study.